

# Circulating Tumor Cell Separation using Circular Reverse Wavy Channel: A Numerical Approach

Submitted By

**Ahmad Jabir**

190011109

**Hamedur Rahman**

190011121

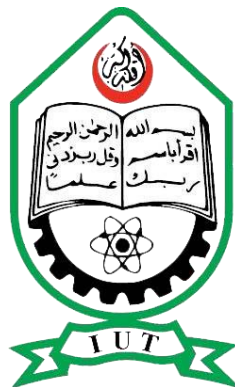
**Rashid Naib Rafi**

190012127

Supervised By

**Prof. Dr. Md. Rezwanaul Karim**

**A Thesis submitted in partial fulfillment of the requirement for the degree of Bachelor of Science in Mechanical Engineering and Industrial and Production Engineering**



**Department of Mechanical and Production Engineering (MPE)**

**Islamic University of Technology (IUT)**

**July, 2024**

## **Candidate's Declaration**

This is to certify that the work presented in this thesis, titled, "Circulating Tumor Cell Separation using Circular Reverse Wavy Channel: A Numerical Approach", is the outcome of the investigation and research carried out by me under the supervision of Prof. Dr. Md. Rezwanul Karim, Professor, Department of Mechanical and Production Engineering, Islamic University of Technology.

It is also declared that neither this thesis nor any part of it has been submitted elsewhere for the award of any degree or diploma.

-----

Ahmad Jabir

Student No: 190011109

-----

Hamedur Rahman

Student No: 190011121

-----

Rashid Naib Rafi

Student No: 190012127

## Recommendation of the Thesis Supervisors

---

The thesis titled “Circulating Tumor Cell Separation using Circular Reverse Wavy Channel: A Numerical Approach” submitted by Ahmad Jabir, Student No: 190011109, Hamedur Rahman, Student No: 190011121 and Rashid Naib Rafi Student No: 190012127 has been accepted as satisfactory in partial fulfillment of the requirements for the degree of BSc. in Mechanical Engineering and Industrial and Production Engineering **on 28<sup>th</sup> June, 2024.**

1.

(Supervisor)

-----  
Prof. Dr. Md. Rezwanul Karim

Professor

MPE Dept., IUT, Board Bazar, Gazipur-1704, Bangladesh.

## CO-PO Mapping of ME 4800 -Thesis and Project

COs	Course Outcomes (CO) Statement	(PO)	Addressed by	
CO1	<u>Discover and Locate</u> research problems and illustrate them via figures/tables or projections/ideas through field visit and literature review and <u>determine/Setting</u> aim and objectives of the project/work/research in specific, measurable, achievable, realistic and timeframe manner.	PO2	Thesis Book	
			Performance by research	
			Presentation and soft skill	
CO2	<u>Design</u> research solutions of the problems towards achieving the objectives and its application. Design systems, components or processes that meets related needs in the field of mechanical engineering	PO3	Thesis Book	
			Performance by research	
			Presentation and soft skill	
CO3	<u>Review, debate, compare and contrast</u> the relevant literature contents. Relevance of this research/study. Methods, tools, and techniques used by past researchers and justification of use of them in this work.	PO4	Thesis Book	
			Performance by research	
			Presentation and soft skill	
CO4	<u>Analyse</u> data and <u>exhibit</u> results using tables, diagrams, graphs with their interpretation. <u>Investigate</u> the designed solutions to solve the problems through case study/survey study/experimentation/simulation using modern tools and techniques.	PO5	Thesis Book	
			Performance by research	
			Presentation and soft skill	
CO5	<u>Apply</u> outcome of the study to assess societal, health, safety, legal and cultural issue and consequent possibilities relevant to mechanical engineering practice.	PO6	Thesis Book	
			Performance by research	
			Presentation and soft skill	
CO6	<u>Relate</u> the solution/s to objectives of the research/work for improving desired performances including economic, social and environmental benefits.	PO7	Thesis Book	
			Performance by research	
			Presentation and soft skill	
CO7	<u>Apply</u> moral values and research/professional ethics throughout the work, and <u>justify</u> to genuine referencing on sources, and demonstration of own contribution.	PO8	Thesis Book	
			Performance by research	
			Presentation and soft skill	
CO8	<u>Perform</u> own self and <u>manage</u> group activities from the beginning to the end of the research/work as a quality work.	PO9	Thesis Book	
			Performance by research	
			Presentation and soft skill	
CO9	<u>Compile and arrange</u> the work outputs, write the report/thesis, a sample journal paper, and present the work to wider audience using modern communication tools and techniques.	PO10	Thesis Book	
			Performance by research	
			Presentation and soft skill	
CO10	<u>Organize</u> and <u>control</u> cost and time of the work/project/research and <u>coordinate</u> them until the end of it.	PO11	Thesis Book	
			Performance by research	
			Presentation and soft skill	
CO11	<u>Recognize</u> the necessity of life-long learning in career development in dynamic real-world situations from the experience of completing this project.	PO12	Thesis Book	
			Performance by research	
			Presentation and soft skill	

Student Name /ID:

Signature of the Supervisor:

1.....

.....

Name of the Supervisor:

2. ....

.....

3. ....

**K-P-A Mapping of ME 4800 -Thesis and Project**

COs	POs	Related Ks								Related Ps							Related As				
		K1	K2	K3	K4	K5	K6	K7	K8	P1	P2	P3	P4	P5	P6	P7	A1	A2	A3	A4	A5
CO1	PO2																				
CO2	PO3																				
CO3	PO4																				
CO4	PO5																				
CO5	PO6																				
CO6	PO6																				
CO7	PO8																				
CO8	PO9																				
CO9	PO10																				
CO10	PO11																				
CO11	PO12																				

Student Name /ID:

1. ....
2. ....
3. ....

Signature of the Supervisor: .....

Name of the Supervisor: .....

## **ACKNOWLEDGEMENT**

In the Name of Allah, the Most Beneficent, the Most Merciful

First of all, we are grateful to ALLAH (SWT), the most benevolent and kind to provide me the strength and ability to write this dissertation. We want to thank our project supervisor, Prof. Dr. Md. Rezwanul Karim, for his strong and patient support through unpredictable problems during the project and his precious advice whenever we faced difficulties. His generosity, kindness and strong supervision during work made us feel less stressed in confronting unexpected troubles and be more productive in our personal life.

We would also like to express our deepest gratitude and acknowledgement to Mr. Sayedus Salehin, Assistant Professor (On Leave), IUT and Doctoral Candidate at the Bilkent University, Turkiye and Mr. Mohammad Raihan Uddin, Lecturer (On Leave), IUT and Graduate Research Associate at the Ohio State University, USA for their unwavering support, invaluable guidance, and encouragement throughout the course of this research without which this research work would not be possible. We are humbled by them making time for advising us while pursuing their own PhD Degrees.

We would also like to thank Mr. Fahim Tanfeez, Lecturer at the Department of Mechanical and Production Engineering at the Islamic University of Technology for his tutorials in generating our results in COMSOL. His insights and feedback have been instrumental in producing quality figures for our results.

On a personal note, we would like to thank our family and friends for their constant support and encouragement. To our parents, for their endless love and belief in us and continued support and dedication towards our higher study, and to our friends, for their patience and understanding during this challenging journey.

## ABSTRACT

Early cancer detection is vital for the survival of a patient suffering from cancers of various types. A study done by the national census for the UK showed that the survival rates of patients suffering from Bowel, Breast, Lung, Ovary, Esophagus, Melanoma decreased from on average of 80% to below 30% for stage 3 cancer and more [1]. Current diagnosis techniques include fresh tissue biopsy, genome sequencing among others which are expensive, require operations to be performed on the patient and could take weeks for the results to arrive. The presence and concentration of Circulating Tumor Cells (CTCs) are key indicators of epithelial cancers, which often release tumor cells into the bloodstream. Current methods include density-based separation via centrifugation and physical filtration using commercial filters. However, these techniques have notable limitations: long processing times, stringent sample preparation to prevent contamination, low CTC recovery, and the need for expensive equipment. Microfluidics offers a promising alternative with simpler devices, faster results, and improved separation. Our design uses the reverse wavy channels from the study published by Zhou et. al [2] and by constraining the entire channel in a circular channel, thus incorporating more turns in the design in a relatively small space, thus potentially reducing costs in manufacturing, smaller overall footprint of the device and reduced pressure losses compared to longer channels. In this study the separation characteristics of CTCs from Blood Cells are analyzed at different Re and at different Aspect Ratios, thus determining the optimum parameters for operation and separation, which show maximum separation occurring at a Reynold's Number of 40 and an Aspect Ratio of 0.32. Furthermore, significant separation is seen to be achieved after 4 reverse wavy channel patterns indicating the number of channel patterns could also be reduced for even smaller footprint of the device. The addition of dielectrophoresis to the existing system could potentially improve the separation and have better sample purity.

# TABLE OF CONTENTS

ACKNOWLEDGEMENT .....	1
ABSTRACT.....	2
TABLE OF CONTENTS.....	3
LIST OF FIGURES .....	5
LIST OF TABLES.....	7
NOMENCLATURE .....	8
CHAPTER 1: INTRODUCTION.....	9
1.1 Background of the Study.....	9
1.2 Problem Statement.....	12
1.3 Goals and Objectives .....	12
1.4 Scope and Limitation of the Study.....	13
1.5 Methodology.....	14
CHAPTER TWO: LITERATURE REVIEW.....	17
2.1 Introduction.....	17
2.2 Microfluidics.....	17
2.3 Inertial Microfluidics .....	18
2.4 Straight Channels .....	19
2.5 Curved Channels.....	20
2.6 Effect of Parameters.....	21
2.7 Patterns and Cross-sectional Development in Spiral-type Channels.....	22
2.8 Similar Curved Channels .....	22
2.9 Reverse Wavy Channel.....	23
2.10 Channels with Contraction-Expansion patterns.....	24
2.11 Hybrid Technologies.....	25
2.12 Cascading Microchannels .....	26
CHAPTER 3: SYSTEM DESIGN AND METHODOLOGY .....	28
3.1 System Design .....	28



3.2 Model Validation: .....	30
3.3 Results for the Computational Model: .....	31
3.4 Study and Analysis for Circular Reverse Wavy Channel .....	32
For Varying Aspect Ratios: .....	32
3.5 Computational Domain: .....	32
CHAPTER 4: RESULTS AND DISCUSSION.....	35
4.1 Grid Independency Test.....	35
4.2 Effect of Varying Aspect Ratios: .....	39
4.3 Effect of Varying Reynold’s Number:.....	44
CHAPTER FIVE: CONCLUSIONS .....	48
5.1 Conclusion .....	48
5.2 Future Scope .....	49
5.2.1 Addition of Hybrid Methods such as integrating Inertial Microfluidics with DEP:.....	49
5.2.2 Cascading Microchannels (Reverse Wavy to Spiral/Contraction-Expansion) .....	49
References.....	50

## LIST OF FIGURES

Figure 1: Superposition of inertial lift flow and dean flow [21].....	11
Figure 2: Reverse wavy channel [2] .....	11
Figure 3: The correlation between particle focusing width and channel Reynolds number in three curved channels utilizing 5 $\mu\text{m}$ and 10 $\mu\text{m}$ particles [15].....	20
Figure 4: The fluid pressure decreases in the three curved channels in accordance with varying Reynolds numbers [15].....	20
Figure 5: Equilibrium Position [21].....	21
Figure 6: Serpentine, square wave and zigzag channel [22].....	23
Figure 7: Three different channel patterns [2] .....	24
Figure 8: Variation of cell separation distance along the width of the outlet against the increase	26
Figure 9: Cascading Channels [50].....	26
Figure 10: Geometric Dimensions of Reverse Wavy Pattern.....	28
Figure 11: Circular Reverse Wavy Channel .....	29
Figure 12: Straight Reverse Wavy Channel.....	30
Figure 13: Separation of Three differently sized particles in Experiment.....	31
Figure 14: Straight Reverse Wavy Channel.....	31
Figure 15: Aspect Ratio .....	32
Figure 16: Mesh for linear reverse wavy channel.....	33
Figure 17: For Coarser mesh (Aspect Ratio = 0.32).....	35
Figure 18: For Coarse mesh (Aspect Ratio = 0.32) .....	36
Figure 19: For Normal mesh (Aspect Ratio = 0.32).....	37
Figure 20: For fine mesh (Aspect Ratio = 0.32) .....	37
Figure 21: For finer mesh (Aspect Ratio = 0.32).....	38
Figure 22: Particle trajectories for Aspect Ratio = 0.25 .....	39
Figure 23: Particle trajectories for Aspect Ratio = 0.27 .....	40
Figure 24: Particle trajectories for Aspect Ratio = 0.30 .....	41

Figure 25: Particle trajectories for Aspect Ratio = 0.32 .....	41
Figure 26: Particle trajectories for Aspect Ratio = 0.36 .....	42
Figure 27: Particle trajectories for Aspect Ratio = 0.39 .....	43
Figure 28: Particle trajectories for Aspect Ratio = 0.40 .....	43
Figure 29: Particle trajectories for Re = 10.....	44
Figure 30: Particle trajectories for Re = 20.....	45
Figure 31: Particle trajectories for Re = 30.....	45
Figure 32: Particle trajectories for Re = 40.....	46
Figure 33: Particle trajectories for Re = 50.....	46

## LIST OF TABLES

Table 1: Simulation Settings -----	14
Table 2: Particle Properties-----	16
Table 3: Channel Dimensions Global Variables-----	30
Table 4: Different Mesh Sizes -----	34

## NOMENCLATURE

CFD	Computational Fluid Dynamics
WBC	White Blood Cell
CTC	Circulating Tumor Cells
DEP	Dielectrophoresis
DLD	Deterministic Lateral Displacement
RBC	Red Blood Cell
FFF	Field Flow Fractionation
$\rho$	Density ( $\text{kg/m}^3$ )
Re	Reynold's Number
De	Dean Number
$F_L$	Lift Force (N)
$F_D$	Dean Drag Force (N)
$a_p$	Particle Diameter ( $\mu\text{m}$ )
U	Velocity (m/s)
H	Height ( $\mu\text{m}$ )
$\mu\text{m}$	Micrometer
$\delta$	Radius of Curvature (m)

# CHAPTER 1: INTRODUCTION

## 1.1 Background of the Study

The ability to control the motion of particles at the microscale is advantageous in various applications. One such application is the controlling the flow of microscale particles using different microfluidic technologies, where channels with dimensions in the micrometer scale, are utilized to identify, sort and/or separate different particles which can be used in biological research and healthcare.

Broadly, microfluidic systems can be classified into two distinct categories:

1. Active Microfluidic System.
2. Passive Microfluidic System.

In active systems, external forces are used to manipulate the particle focusing and separation however, the throughput in the active system is low. Here particles are separated through using Field-Flow-Fractionation techniques where an external field is used to manipulate and direct the motion of particles across the channel cross-section. Active systems include dielectrophoresis, magnetophoresis and acoustophoresis, where particles re separated based on the forces they experience due to different dielectric, magnetic properties etc. [3]. Active Systems are generally costlier and more complex compared to passive systems due to their use of external devices to generate, sustain and tune those forces. On the other hand, passive systems do not use any external forces to manipulate particle sorting and cell separation. It is simple, cheap, high precision and it deals with high throughput. Some passive systems are deterministic lateral displacement [4], inertial microfluidics etc. In passive system it basically includes the separation based on size [5].

Due to its simplicity and high throughput passive system is becoming very popular in the field of microfluidics [6]. Inertial microfluidic systems use no external source for particle manipulation for sorting and separation it solely depends on the inertia of the fluid [7], [8]. Purely hydrodynamic forces are used to direct cells/particles. Inertial Microfluidics operates at relatively low Reynold's numbers ( $1 < Re < 100$ ) [9]. Within this range, particles can flow through lateral migration (inertial

migration) or generate secondary flow (transverse flow). Inertial migration occurs when particles migrate laterally due to inertial lift force ( $F_L$ ), which is a combination of:

1. Shear gradient lift force ( $F_{LS}$ )
2. Wall-induced lift force ( $F_{LW}$ )

The lift force,  $F_L$ , that scales as: [10], [11], [12], [13], [14]

$$F_L \propto \rho U^2 \frac{a^4}{H} \quad (1)$$

Particles in microchannels typically exhibit a profile of parabolic velocity, with the relative velocity of the particle on the side of the channel wall is greater than the center velocity of the channel[15]. This pressure difference generates a wall-directing force, known as the shear gradient-induced lift force ( $F_{LS}$ ). When a particle comes near to the channel wall, it generates a center-directing force through interaction with the wall ( $F_{LW}$ ) [16]. Particle confinement and a curved velocity profile are required for observing inertial particle migration.

The equilibrium position is then determined by the combined effect of these two forces. For the equilibrium position, particle tends to sort in the annulus of the geometry[17]. Finite element solutions to incompressible systems The Navier-Stokes Equations resulted in a unique scaling of lift force, which was also affected by particle location in the channel[18], [19].

To achieve success, the size of particles must be equivalent towards behavior of channel dimension and the ratio must exceed 0.07. A secondary flow is growing up when an inert fluid passes through curved microchannels, in Figure 1 producing a radial pressure gradient for the profile of parabolic velocity. Dean flow intensity in a curved channel in figure 1 is quantified by Dean number: [20]

$$\text{Dean number, } De = \left(\frac{H}{2R}\right)^{\frac{1}{2}} \times Re \quad (2)$$

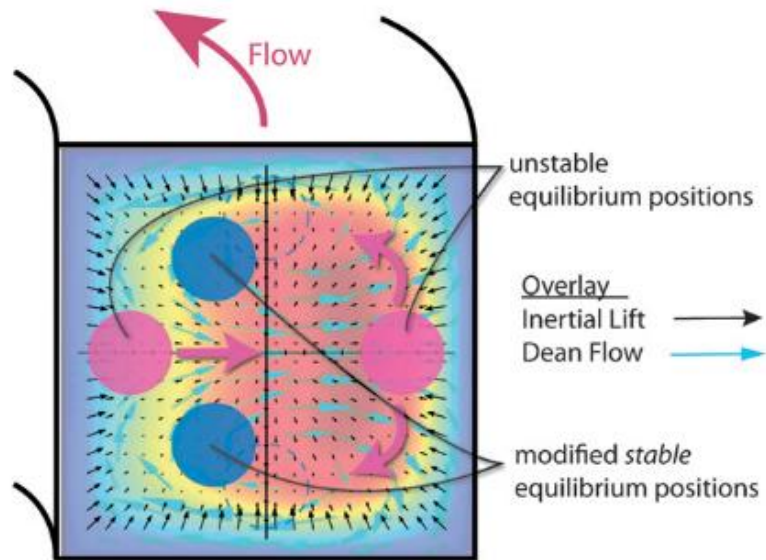


Figure 1: Superposition of inertial lift flow and dean flow [21]

A new channel is emerged which is called reverse wavy channel. In this reverse wavy channel design, in Figure 2 there is four semicircles. And it has also sharp turns. These geometric design helps to focus even the smallest of the particle smoothly.

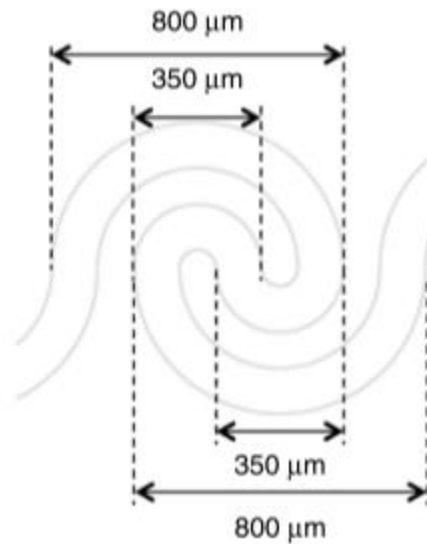


Figure 2: Reverse wavy channel [2]



## 1.2 Problem Statement

Inertial Microfluidics presents some key challenges:

- One of the most complicated problems is overlapping. Particles of almost similar sizes tend to sort at the same equilibrium position.
- Particles of small diameter are very difficult to separate, such as the platelets which is only 3  $\mu\text{m}$ .
- Channel length may complicate the focusing or separation operation.

To improve the separation,

- A more refined design is needed which will contain more turns and will help focus even the smallest of the particles smoothly. This is where the reverse wavy channel comes in. It contains four semicircular points which introduces more turns in a compact space and also solves the problem of separation and overlapping.
- The reverse wavy channel contains sharp turns which will help to focus the smallest of the particles, for example - platelets.
- Aspect ratio will be kept below '1' which will not shorten the length of the channel and particles will have sufficient distance to settle in the equilibrium position.

## 1.3 Goals and Objectives

Objectives:

- To separate Circulating Tumor Cells from blood cells using **Inertial Microfluidics** with maximum separation distance
- To Optimize for the varying:
  - Reynold's Number
  - Aspect Ratio

- To Analyse Separation Performance based on Lateral Separation Distance and focusing of particle streams using:
  - Particle Trajectories
  - Velocity Contours/Plots

#### **1.4 Scope and Limitation of the Study**

The use of Reverse Wavy Channels in sheath less separation is comparatively a new phenomenon and has not been explored to the required state. Though there is some numerical and experimental works have been conducted, it has a long way to go.

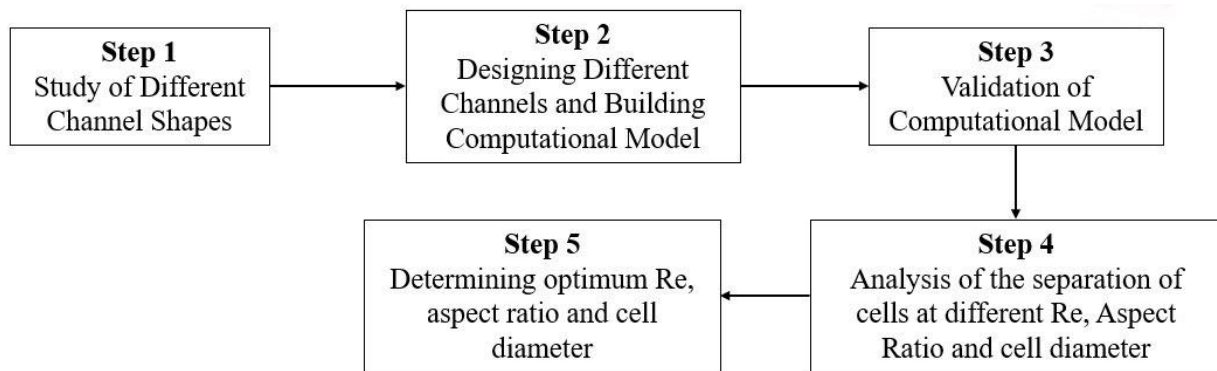
As the inertia effect and the dean effect increases for more turns a new channel shape is introduced by merging Reverse Wavy patterns with a Circular Shape. This allows separation of cancer cells without the use of sheath flows.

Limitations-

- Overlapping of similarly sized particles cannot be determined through computational analysis.
- Conventional Laboratory tests require expensive hardware to accurately conduct tests.

## 1.5 Methodology

In the flow chart we have described the sequence of our work. In this research, firstly, the different channel shapes to be implemented in our design for effective separation were analyzed. This was done by studying literature on various channel shapes and their effects on dean flow and consequently separation. After that, a computational model was built on COMSOL to simulate the flow of the blood cells and circulating tumor cells in the channel. This computational model was validated by an experimental paper by Zhou et al. [22].



After the validation, the separation of cells at different Aspect Ratio, Reynold's Number and Cell Diameter was analyzed to find the optimum configuration for maximum separation.

**Table 1: Simulation Settings**

Procedure	Element
Import	As file type IEGS (.igs)
Material	Liquid, Water
Add Physics	Fluid Flow - Single Phase - Laminar
Discretization of Fluids	<b>P2+P2</b>

Fluid Properties	All from the material
Wall	No Slip Boundary Condition
Inlet Velocity	0.86 m/s
Mesh	Sequence Type: Physics-Controlled Mesh (Laminar Flow) Element Size: Coarser (Test Run with Extremely Coarse) (Wavy 0.8 7-8, Complete mesh consists of 14342 domain elements, 4620 boundary elements, and 1352 edge elements) Tetrahedral
Stationary Study	Initialization for velocity field plots computation time: 22s
Add Physics	Particle Tracing for Fluid Flow
Velocity	Velocity Field
Drag Force	Drag Law: Stokes Velocity: Velocity Field
Wall Induced Lift Force Up Down	Lift Law: Wall Induced (not Saffman because too low) Select parallel Boundaries (Top and Bottom) Velocity: Velocity Field Dynamic Viscosity: Dynamic Viscosity (spf/fp1)
Wall Induced Lift Force Side Walls	Lift Law: Wall Induced (not Saffman because too low) Select parallel Boundaries (Side Walls) Velocity: Velocity Field Dynamic Viscosity: Dynamic Viscosity (spf/fp1)
Outlet	Wall Condition: Freeze
Add Study	Time Dependent: Time Range: 0 to 2 seconds (2s is time taken for particles to go from inlet to outlet) with 0.01s time step (we will do 0.1s time step, to save computational time; test run, and 0-2s total time) Tolerance: Physics Controlled Physics and Variables Selection: Only particle tracing Values of Dependent Variables: Values of Variables not solved for: User Controlled, Method: Solution, Study: 1-VF, Stationary

**Table 2: Particle Properties**

<b>Particle</b>	<b>Properties &amp; Release Time</b>
RBC	Density: 1050 kg/m <sup>3</sup> Diameter: 6 μm Release Time: 0.01 s
WBC	Density: 1050 kg/m <sup>3</sup> Diameter: 10 μm Release Time: 0.02 s
CTC	Density: 1050 kg/m <sup>3</sup> Diameter: 20 μm Release Time: 0 s

## **CHAPTER TWO: LITERATURE REVIEW**

### **2.1 Introduction**

The basics of microfluidics and the types of system in microfluidics were studied. Firstly, active and passive systems were studied in detail. Active systems are where there is an external force or force field used to influence the trajectory of microparticles. Whereas, passive systems do not use any external forces to do so. To overcome certain shortcomings a new system called hybrid system can be used where both active and passive systems are used to better separate or focus the particles and in this case the throughput is also higher. One such passive system used is Inertial microfluidics, where particles are separated or focused based on hydrodynamic effects only, due to the inertia of the particles. After analyzing systems, different several channel shapes and geometries were studied and their effects on the particles movement. In straight channels where the particles are sorted based on the inertial effect, in curved channels a new flow is generated which is called secondary flow or Dean Flow which is perpendicular to the direction of flow of particles, along the channel cross-section. Some other similar curved channels include the serpentine channel, square wave channel and zigzag channel [23]. One such interesting channel is the reverse wavy channel [2]. Articles from various journals and publications including renowned journals like Lab on a Chip from the Royal Society of Chemistry, Micromachines, Scientific Reports from Nature, Chemical Engineering Science, Annual Review of Biomedical Engineering, Microsystems and Nanoengineering, Biotechnology Progress etc. have been studied for a comprehensive literature review.

### **2.2 Microfluidics**

In microfluidics we deal with two types of systems. They are-

1. Active system
2. Passive system.

In active system there is external effect which is manipulating the particle separation and focusing. And on the passive system there is no external effect present. The example of active system is

dielectrophoresis [24], [25], [26], magnetophoresis, acoustophoresis[27], [28]. And the example of passive systems is deterministic lateral displacement [29], inertial microfluidics. There is a problem regarding the throughput and the overlapping of the similar sized particles while separating which can be solved by using hybrid system such as integrating dep with inertial microfluidics [30].

### 2.3 Inertial Microfluidics

In particle focusing or separation the inertial effect is usually ignored. But when we look at the particle it has certain flow rate which means it has some velocity. That means the flow has certain Reynolds number. From the definition of Reynolds number,

$$Re = \frac{\text{Inertia Force}}{\text{Viscous Force}} \quad (3)$$

This inertial effect helps to sort particle according to the sizes of the particle diameter [21]. This has two components:

1. Wall induced lift force
2. Shear gradient lift force.

The equilibrium position is the result of these two combined forces[31]. Rectangular microchannels utilized in the manipulation of inertial particles can be defined into the following categories: expansion-contraction, spiral, linear, and sinusoidal. Channel structures have found wider applications in the fields of biology, medicine, and industry due to recent developments. The innovation of 3D printing and the advancement of micromachining technology have simplified the 3D microchannels into inertial microfluidics.

Gossett and Di Carlo (2009) demonstrated a paper about focusing and separation of particles in curving confined flows. In inertial microfluidics normally particle will focus at an equilibrium position due to the inertial lift force. If the geometry has curves, then the particle will not focus into a position just based on the inertial lift force. For curved segments secondary flow will be generated. So, this will affect the equilibrium position. The ratio of inertial lift to dean drag force will determine the equilibrium position in a curved channel. Also, the ratio depends on the various

Reynolds number ( $10 < Re < 100$ ). [14] There are several types of separation in inertial microfluidics, such as separation based on particle size [32] [33] [34].

## 2.4 Straight Channels

In straight channel the particles are affected only by the lift force that works perpendicular to the flow of the particle. In a square shaped channel, the equilibrium position is four where in the rectangular channel the equilibrium position is two [31], [35], [36], [37].

The location and quantity of the ultimate equilibrium positions are determined by the microchannel's cross-section. Particles flow laterally through circular sections to generate an annulus having an average radius that is 0.6 times of that channel. In rectangular sections defined by high or low aspect ratios, due to the substantial difference in shear gradient between the long and short channel walls, the two equilibrium locations on the short walls are rendered unstable. As a result, particles are confined to two equilibrium positions of the middle portion of the long channel walls.

The particles are kept in a straight channel at equilibrium locations by these lift forces. However, inertia modifies the Dean flow's initial equilibrium states. Because  $R_f$  is diameter-dependent, particles of different sizes can be categorized to different forces and separated inside the same spiral channel. Particle enrichment and separation have made extensive use of spiral rectangular channels with a high area ratio (LAR). Bhagat et al., for instance, reported the successful separation of polystyrene particles with diameters ranging from 1.9 to 7.32 micrometers inside a spiral microchannel with five loops.

In Figure 3 the variability of focusing width with the channels Reynolds number is discussed for three different channels. And in figure 4 the variation of pressure drop is discussed with the Reynolds number for three different channel (serpentine, square wave and zigzag channel) shape.



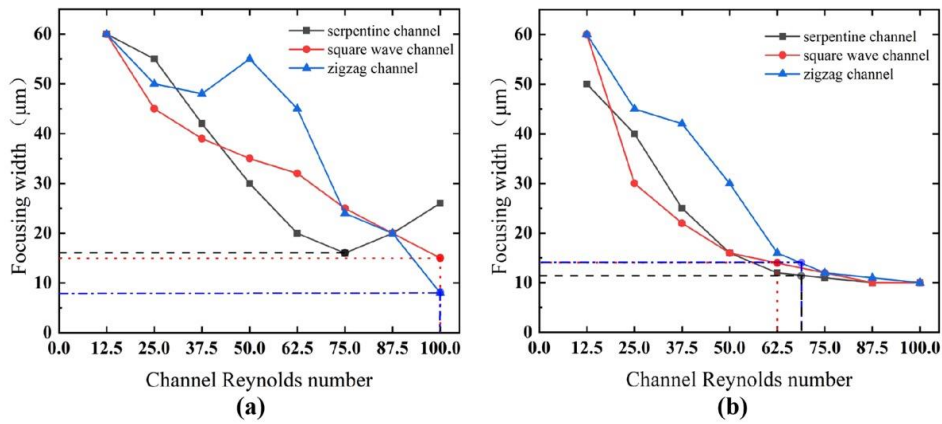


Figure 3: The correlation between particle focusing width and channel Reynolds number in three curved channels utilizing  $5 \mu\text{m}$  and  $10 \mu\text{m}$  particles [15]

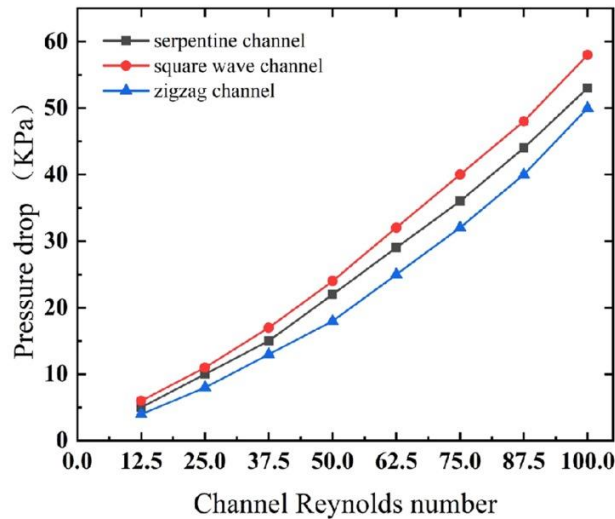


Figure 4: The fluid pressure decreases in the three curved channels in accordance with varying Reynolds numbers [15]

## 2.5 Curved Channels

In curved channel the path is not uniform as straight channel. So, there will be mismatch in velocity in the different points in the channel. This mismatch velocity creates a flow in the cross-sectional lateral direction which is called secondary flow. It creates vortex in the channel. And because of the effect of secondary flow a new equilibrium position in Figure 5 is formed[31]. The ratio of inertial force to dean drag force is very important for the sorting of particles[27],[28].

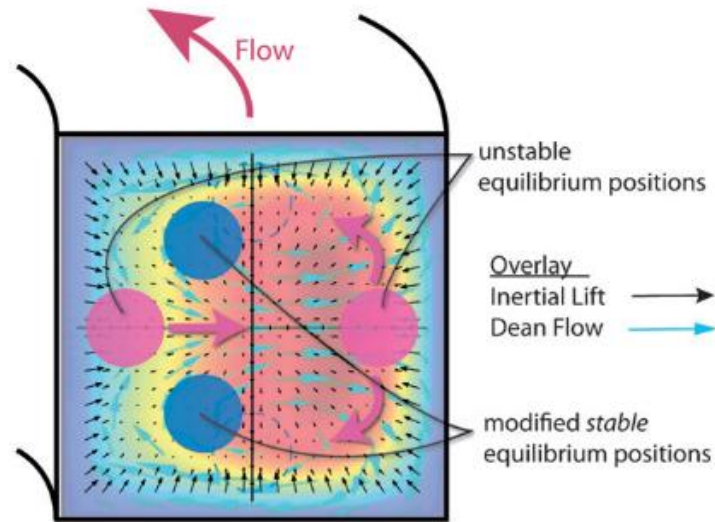


Figure 5: Equilibrium Position [21]

## 2.6 Effect of Parameters

The effect of Reynolds number; [40] [41] If the Reynolds number is raised, the equilibrium position shifts to the wall. In rectangular channels it will create four equilibrium position instead of two. The equilibrium position depends on particle size. If  $a/H$  ratio approaches 1 then the particle will move to the channel center [31] (Zhou et al. 2013). demonstrated a paper for the separation in an inertial microfluidics system which employs two stage inertial migration. One of the drawbacks of the inertial microfluidics is the efficiency and purity issue of the separated cells. In this paper the system achieves the efficiency of 99% and also purity greater than 90%. In the separation they manipulated the result by modulating the aspect ratio of the channel geometry. For the optimum aspect ratio, they achieved the complete separation. And also, while getting the complete separation throughput of the system was not compromised. They have done the separation for various Reynolds number for different aspect ratio. For certain Reynolds number they have increased and decreased the aspect ratio. They got complete separation at  $Re = 40$  [20].

Larger cells are concentrated to the channel center in a linear microchannel with a high aspect ratio (HAR), while smaller cells become more concentrated near the channel wall following an extended distance of flow.

## 2.7 Patterns and Cross-sectional Development in Spiral-type Channels

With its constant-direction curvature, the spiral channel is a popular choice for implementing inertial effects while reducing the microfluidics device's size and channel length. Due to the superposition of inertial lift and Dean drag force, particles in a spiral channel are stabilized at specific equilibrium coordinates inside the channel's cross-section. The relationship between those two forces in terms of their magnitudes determines the final particle focusing characteristics. When  $R_f$  becomes close to zero, particle passes within the Dean flow occur, and the behavior of the substances is revealed by the Dean drag force. The inertial lift forces take the role of the Dean drag force when the magnitude of  $R_f$  increases. The particles are kept in a straight channel at equilibrium locations by these lift forces. However, inertia modifies the Dean flow's initial equilibrium states. Because  $R_f$  is diameter-dependent, particles of different sizes can be categorized to different forces and separated inside the same spiral channel. Particle enrichment and separation have made extensive use of spiral rectangular channels with a high area ratio (LAR). Bhagat et al., for instance, reported the successful separation of polystyrene particles with diameters ranging from 1.9 to 7.32 micrometers inside a spiral microchannel with five loops [16].

## 2.8 Similar Curved Channels

In a channel when the particles are interacting with the flow shear gradient lift force directs the particle away from the channel center and on the other hand the wall induced lift force directs the particle away from the channel wall. When these two forces equal an equilibrium position is created for the particles. In the paper [23], serpentine channel, square wave channel and zigzag channel in Figure 6 is compared for the focusing and separation operation. For the separation performance zigzag channel is the best at  $Re=62.5$ . It shows a separation distance of  $10\mu m$ . Also, for the focusing application zigzag channel gives the best result among these three channels. We can see that there is an issue regarding the Reynolds number. Serpentine channel and square wave also produce the optimum separation and focusing but after a certain limit ( $Re > 75$ ) zigzag channel produces the best result.

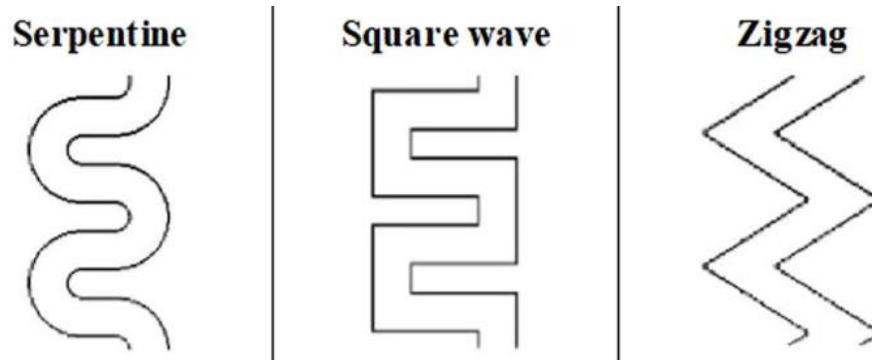


Figure 6: Serpentine, square wave and zigzag channel [22]

## 2.9 Reverse Wavy Channel

A group of reverse wavy channel topologies are built into the channel design to enable the process of concentrating and sorting cells without the need for a protective covering. A solitary undulating channel piece of four semicircular segments that generate on an ongoing basis inverted Dean secondary flow over the channel's cross-section. Deterministic equilibrium focusing sites arise from the equilibrium within the inertial lift force as well as the Dean drag force[42]. The stability of this equilibrium is contingent on the dimensions of the particles and cells passing through the flow. An investigation was conducted on the behavior of inertial focusing, which is dependent on the size of the particles[43]. Fluorescent microspheres of six various sizes (15, 10, 7, 5, 3, and 1  $\mu\text{m}$ ) were used for this purpose. Our innovative design, consisting of subunits with exceptional maneuverability, can efficiently concentrate particles which can be at least 3 $\mu\text{m}$ , which is the median measurement of platelets. This enables the effective isolation of cancer cells from the entire bloodstream where it doesn't require the sheath flows. We successfully sorted MCF-7 cancer cells in adulterated whole blood specimens with respect to their size, without the need for sheath flows. Adopting an improved channel design helped to achieve this. A total of 89.72% of the MCF-7 cells were successfully isolated from the initial mixture in a single sorting operation. Furthermore, the purity of the cells improved to 68.9%, resulting in a significant enrichment. Importantly, the sorted cells exhibited high vitality.

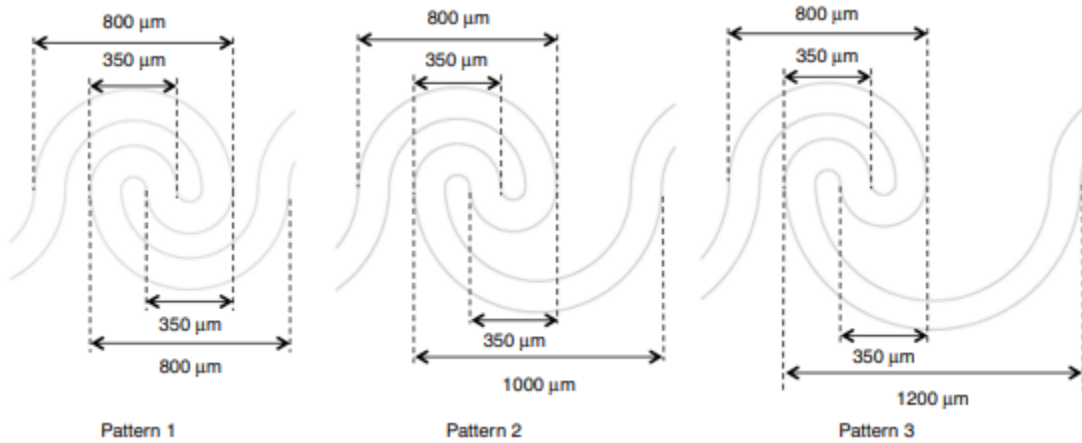


Figure 7: Three different channel patterns [2]

The channel designs have 125  $\mu\text{m}$  of width and a height of 40  $\mu\text{m}$  of height and it has three patterns as Figure 7. With a volumetric rate of  $3.29 \cdot 10^{-9} \text{ m}^3/\text{s}$ , the input velocity was calculated, corresponding to a channel Reynolds number ( $Re_c$ ) of 40. Furthermore, the maximum speed of the Dean flow was also established. A precise volumetric rate of  $3.29 \cdot 10^{-9} \text{ m}^3/\text{s}$ , or a Reynolds number ( $Re_c$ ) of 40, was used for each simulation. A flow profile is shown along the channel's cross section; the left and right sides represent the inner wall, which has a smaller curvature radius, and the outer wall, which has a larger curvature radius. The fluid's inertia becomes substantial in a Reynolds number domain that is intermediate, with values ranging from around 100 to approximately 1, when it flows through a turning channel. The fluid with higher velocity in the central region of the channel tends to go in the direction perpendicular to the cross-section, towards the outside wall, following the main flow direction. To keep the total mass of the fluid in the constrained channel, the fluid with lower velocities at the top and lower walls seeks to migrate towards the inner wall. The aforementioned occurrence produces two symmetrical vortices that rotate opposed to the main flow direction in opposing orientations. The Dean secondary flow is the term used to describe the vortices.

## 2.10 Channels with Contraction-Expansion patterns

To incorporate convective secondary flow, a tube with alternating contracting and expanding is used[44]. Centrifugal forces during this process produce a secondary vortical flow in the transverse

plane. This secondary flow causes the boundary to separate in the expansion region, ultimately giving rise to a micro vortex in the horizontal plane. Consistently directing and arranging microparticles in either the center or periphery areas was the accomplishment of Park et al [17]. The utilization of multi-orifice flow fractionation (MOFF) was suggested to enhance the coverage yield while reducing purity loss.[45] It was shown that biological cells can be changed successfully by separating leukocytes and erythrocytes, adding malaria parasites to the blood, and continuing to separate human breast cancer cells (MCF-7) from a sample of primed blood cells. Micro Vortices that situated in areas of high flow rates and expansion are good at catching particles in Figure 8, this implies that they have the capability to be used for solution exchange, cell concentration, and sorting cells by size. A lot of researchers have come up with hybrid devices that can trap cells by combining different structures that expand and contract. It can be seen in the "Centrifuge-on-a-Chip" developed by Mach et al [18]. The technology separated and enriched cancer cells from those blood samples using an expansion-contraction chamber and a linear HAR channel. In order to successfully separate cancer cells from blood samples, Sollier et al. presented a modified Vortex chip and created concurrent multiple trapping arrays in their investigation [19]. Zhou et al. utilized experimental measurements and numerical simulation to examine the impact of flow conditions, the size of trapping region, and target particle which have concentration on the trapping behavior [20].

## **2.11 Hybrid Technologies**

Hybrid Technologies in inertial microfluidics is not exactly in the arena of passive microfluidics as it uses external forces/fields to direct cells[46]. However, as they implement the use of passive systems such as inertial microfluidics to a great extent, they fall under the category of "hybrid" systems[47].

(Islam and Chen 2023) demonstrated a solution for the overlapping issue that we face while separating circulating tumor cells from the white blood cell. The overlapping issue is when we deal with the white blood cell of various sizes. For efficient separation, they coupled dielectrophoresis with the inertial microfluidics. Combining these both will help us to overcome both overlapping issue and throughput issue. At first, they determine the optimum CE sections for

the best separation. The best separation they got when they used 7 sections. Then they conducted the DEP operation. The overlapping issue was solved at 50V for which they got the separation distance of 233.4  $\mu\text{m}$  [21].

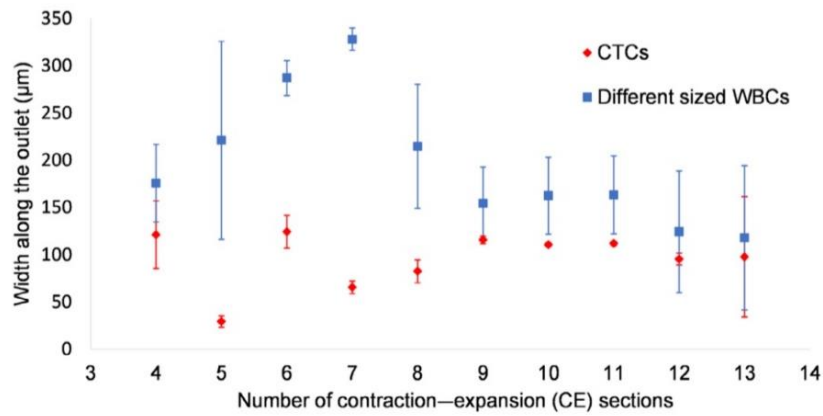


Figure 8: Variation of cell separation distance along the width of the outlet against the increase

## 2.12 Cascading Microchannels

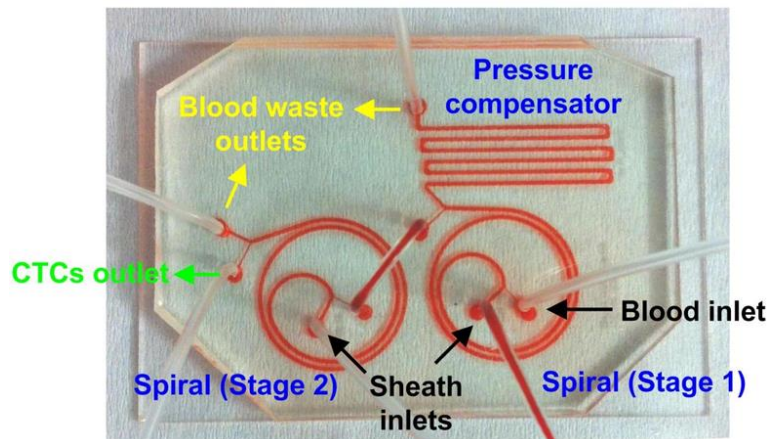


Figure 9: Cascading Channels [50]

Cascading microchannel in Figure 9 is the combination of two or more same or different microchannels. The main channel can be into multiple smaller channels having a specific width

and dimension. As the fluid flows through the channel the larger particles are directed into wider channels because of their size on the other hand smaller particles flow into narrower channels. Compared to other complex microfluidic separation techniques, cascading microchannels are relatively easy to fabricate and operate.



## CHAPTER 3: SYSTEM DESIGN AND METHODOLOGY

### 3.1 System Design

The research design incorporates a reverse wavy microchannel in, which is a novel channel pattern for separating circulating tumor cells (CTCs). The microchannel's unique wavy characteristics are designed to maximize fluid dynamics, which will facilitate effective and high-yield CTC separation. This novel design has the potential to improve CTC separation methods' precision and efficacy, advancing cancer research and opening the door to more targeted treatment and diagnostic approaches. The experimental model of the existing literature and the numerical model of Yinning Zhou, Zhichao Ma, and Ye Ai have both been validated, as has the novel channel. They produced and effectively separated the larger particles from the upper outflow, while the remaining particles were separated in their reverse wavy channel.

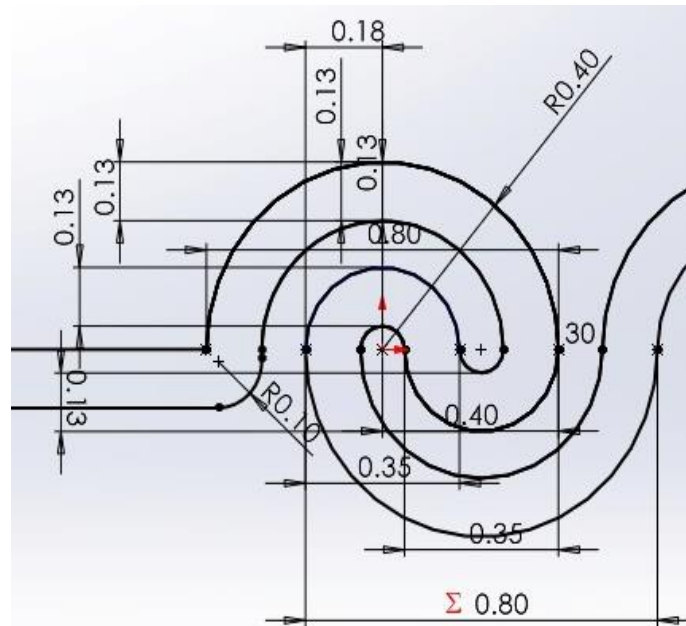


*Figure 10: Geometric Dimensions of Reverse Wavy Pattern*

The microchannel was composed of thirty reverse wavy channels Figure 12, with the radius of curvature of the lower outer semicircle ranging from 100 to 200  $\mu\text{m}$ . In three patterns, the channel designs have a width of 125  $\mu\text{m}$  and a height of 40  $\mu\text{m}$  as shown in Figure 10.

Separation was achieved Figure 13 by employing the same focal geometry in a curvilinear manner (Figure 11), as opposed to the linear version. The dimensions have been maintained at constant height and breadth. The rounding diameter of another channel named contraction expansion channel was utilized to round the geometry [48], and the results were way better to those of the linear channel.

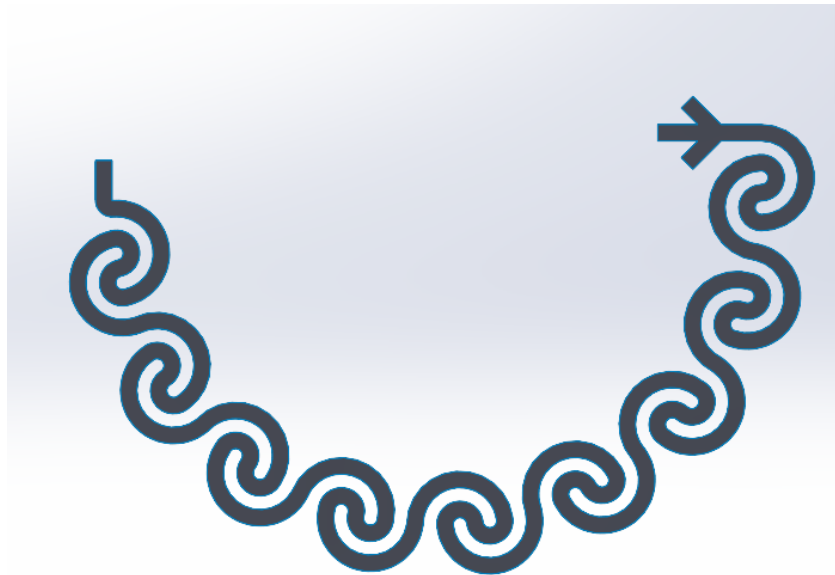


*Figure 11: Circular Reverse Wavy Channel*

There were discontinuities at two adjacent channels and errors regarding the outflow geometry during the microchannel's normalization process. Particles were effectively separated in the proposed novel geometry by resolving all of those issues. The aspect ratio and  $Re$  was varied to achieve improved separation.

### 3.2 Model Validation:

- The reverse wavy microchannel (linear) design is based on the published paper Zhou Y et al. *Microsys. and Nanoengg.*, vol. 4, Issue 1, 2018. The **circular channel** is the proposed design for analysis.
- A three-dimensional CFD model has been computationally simulated in COMSOL Multiphysics 6.1.
- CAD designed on SolidWorks 2023

All the channel designs have a width of 125  $\mu\text{m}$  and a height of 40  $\mu\text{m}$ .

**Table 3: Channel Dimensions Global Variables**

Global Variables	Value	
a	0.125	0.125 mm
b	0.8	0.800 mm

Here 'a' is the distance between two wavy channels.

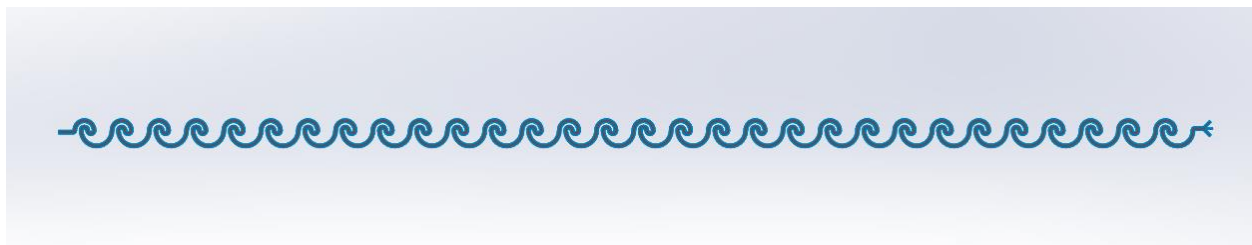


*Figure 12: Straight Reverse Wavy Channel*

A computational fluid dynamics model of the Linear Reverse Wavy Microchannel was simulated on COMSOL and it showed similar results with that of the experimental results of Zhou et al.

In the **Experimental** Results from the paper:

- The 10  $\mu\text{m}$  particle separated in to the Output 1/Upper outlet
- The 15  $\mu\text{m}$  particle separated in to the Output 2/Middle outlet
- The 3  $\mu\text{m}$  particle separated in both Output 3/ Lower outlet

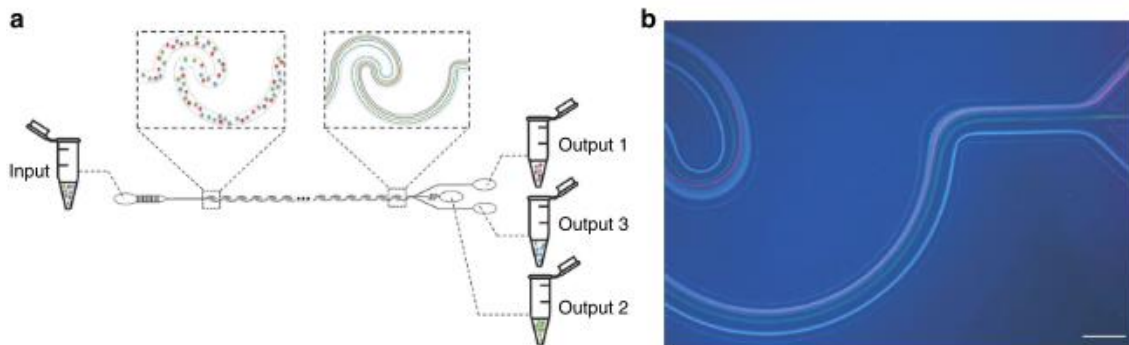


Figure 13: Separation of Three differently sized particles in Experiment

### 3.3 Results for the Computational Model:

We obtained separation of particles similar to that in the experiment carried out by Zhou et al. with all three particles in different channels as shown in the Figure 14 below.

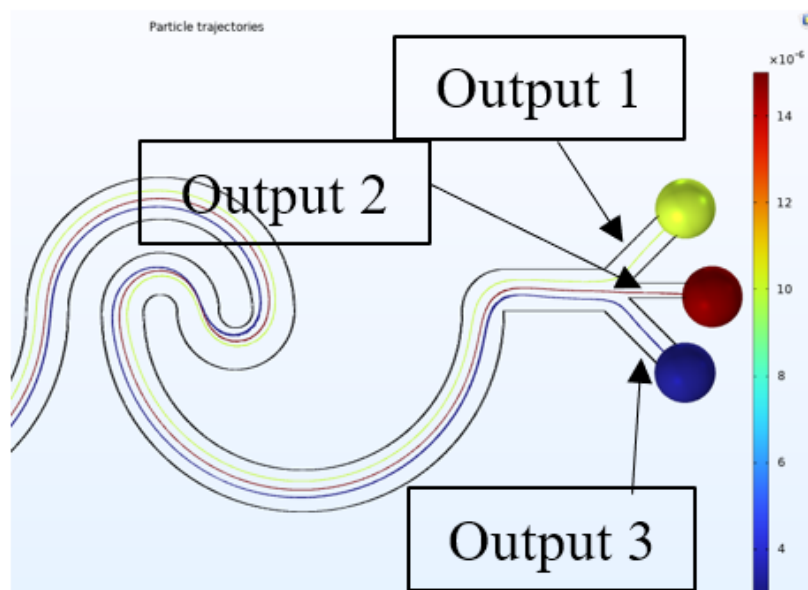


Figure 14: Straight Reverse Wavy Channel

Thus, the computational model can accurately represent the separation of particles in the experiment with the three particles in three different channels.

This model could now be used to analyze different scenarios including reverse wavy channels now and study their separation.

### 3.4 Study and Analysis for Circular Reverse Wavy Channel

#### For Varying Aspect Ratios:

The channel aspect ratio detailed in Figure 15 or the ratio of the height/width (H/W) (Figure 15) of the channel cross-section is to be varied from 0.25 – 0.40 and the channel with the largest lateral separation of particles (CTCs and RBC & WBC) across the width of the cross-section is to be chosen for further analysis.

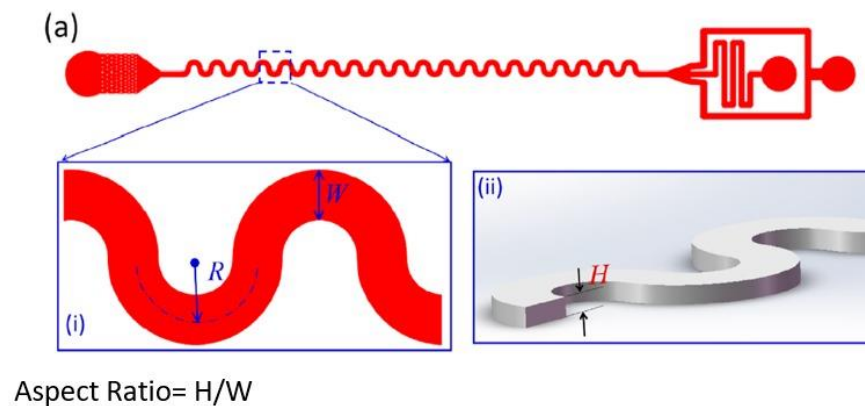


Figure 15: Aspect Ratio

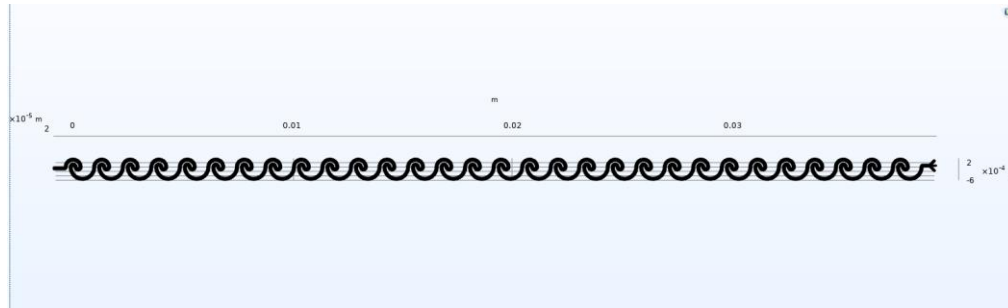
#### 3.5 Computational Domain:

Extra Coarse, Coarser, Coarse, Normal, Fine, Finer

Domain Elements: 18478

Boundary Elements: 6008

Edge Elements: 1690

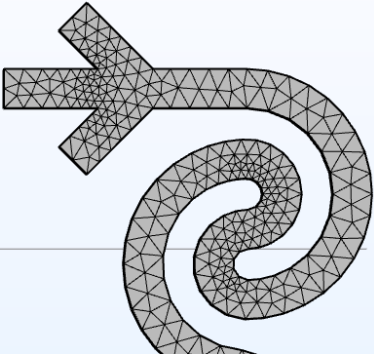
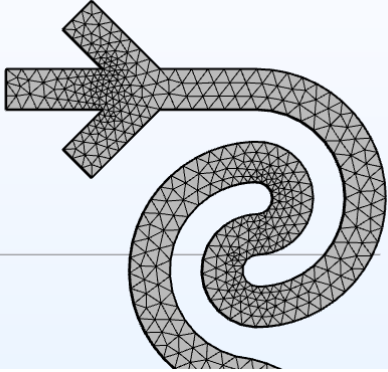
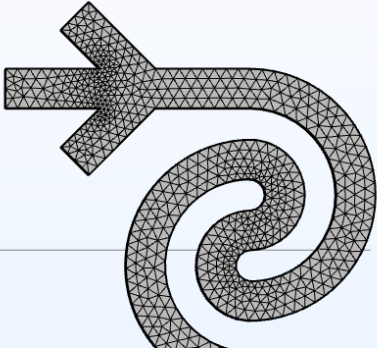
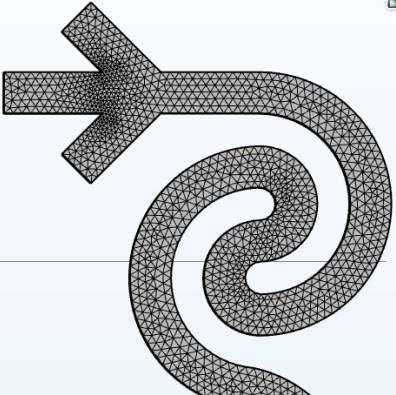
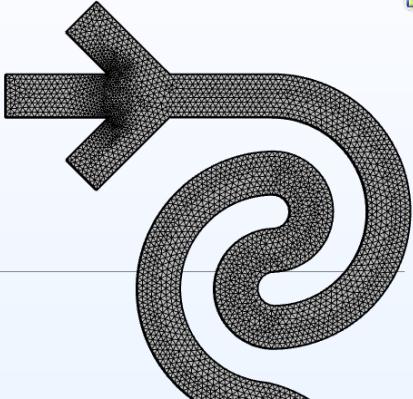


*Figure 16: Mesh for linear reverse wavy channel*

The design of the linear reverse wavy channel was improved by adding curves to the design of the microchannel. Inherently, the reverse wavy channel has four semicircular segments which helps to focus even the smallest of the particles because of the dean flow dominating the inertial lift forces in case of the smallest particles. More curves were added to the geometry so that the dean flow dominates the inertial lift forces and we get the highest distance between the large and small sizes particles. As the objective was to separate the circulating tumor cells from the rest of the blood cells, we can use this advantage because CTCs are the biggest particle present in the blood sample.

For best results different kinds of mesh as in Figure 16 were utilized for the new geometry. Starting from the extra coarse and upgrading it gradually until the finer mesh size. As the geometry possesses sharp turning thus finer mesh sizes are implemented on those areas to get the best result.

**Table 4: Different Mesh Sizes**

Coarser	Coarse	Normal
 A 2D mesh of a complex shape with a horizontal bar on the left and a curved tail on the right. The mesh is composed of large, coarse triangular elements.	 A 2D mesh of the same complex shape as the 'Coarser' mesh, but with smaller, more uniform triangular elements.	 A 2D mesh of the same complex shape, with a significantly higher density of small triangular elements compared to the 'Coarse' mesh.
Fine		Finer
 A 2D mesh of the complex shape with a very high density of small triangular elements, appearing as a dark, almost solid area.		 A 2D mesh of the complex shape with an even higher density of small triangular elements than the 'Fine' mesh, making it appear even darker and more solid.

## CHAPTER 4: RESULTS AND DISCUSSION

For the analysis of our geometry of circular reverse wavy channel we have taken three particles of  $5\ \mu\text{m}$  (Red blood Cell),  $10\ \mu\text{m}$  (White Blood Cell),  $15\ \mu\text{m}$  (Circulating Tumor Cell). Particles will be released one after another. Firstly, RBC will be released at the beginning. After that, at  $0.01\text{s}$  WBC will be released finally at  $0.02\text{s}$  CTC will be released. 4 particles of each type will be released

### 4.1 Grid Independency Test

At first, the extra coarse mesh as seen in Figure 17 is used to see if the simulation settings are valid or not. After that, the mesh will be gradually made finer to check if the results are same or different for different meshes. If the results are same for different meshes than the grid independency will be achieved.

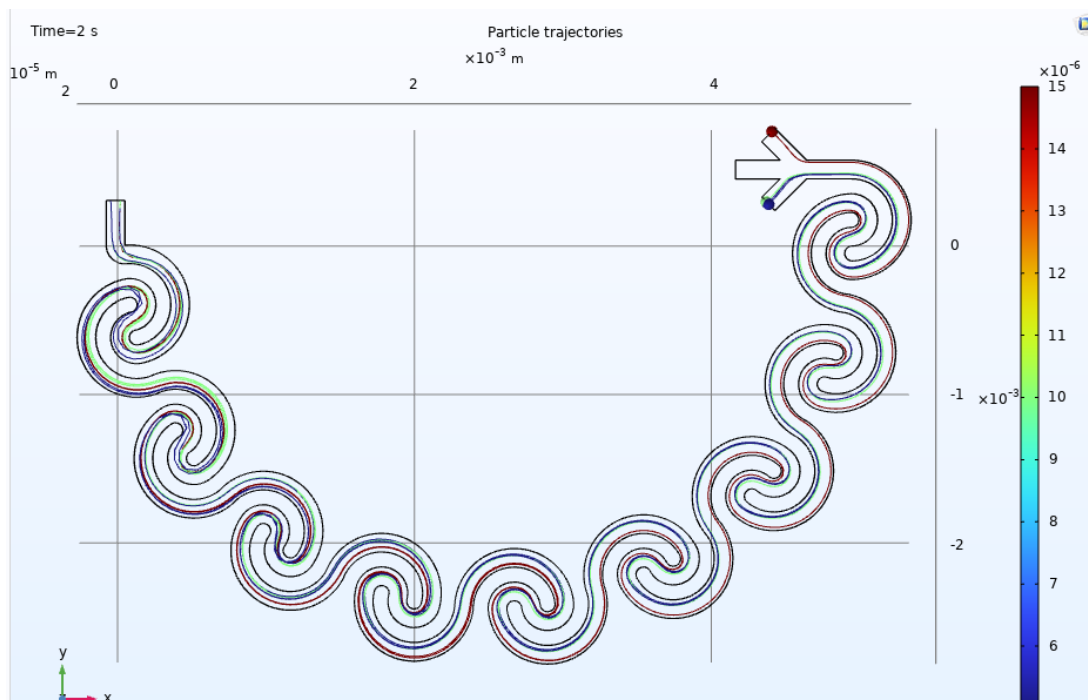


Figure 17: For Coarser mesh (Aspect Ratio = 0.32)



From the results of the simulation, the circulating tumor cells are seen to be separated from the rest of the blood. A large gap is achieved between the CTC particles and the RBC and WBC particles. From the simulation result it can be deduced that the larger particles are going through the upper outlet and the rest of the particles are going through the lower outlet.

- CTC Separation with Circular Reverse Wavy Microchannels.
- Separation was achieved at the outlet with the RBCs and WBCs in one outlet channel and CTCs in the other.

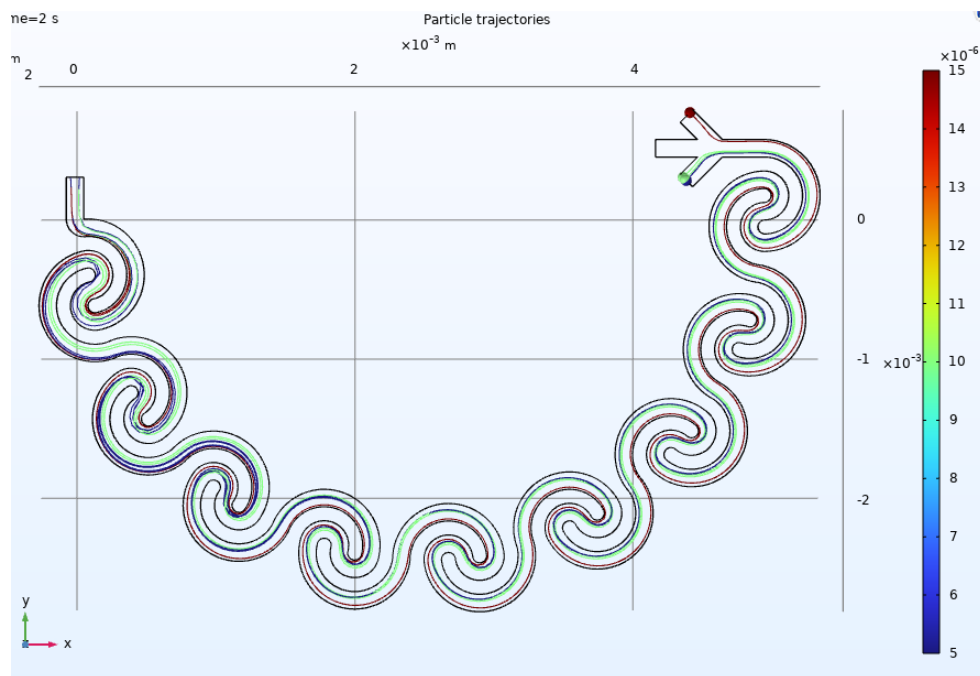


Figure 18: For Coarse mesh (Aspect Ratio = 0.32)

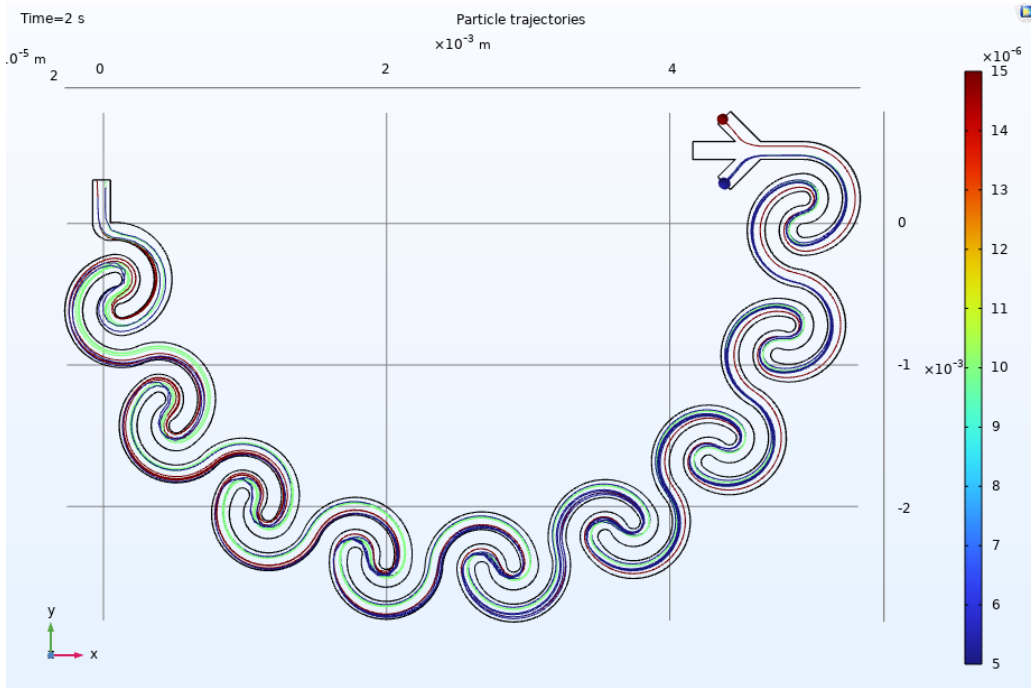


Figure 19: For Normal mesh (Aspect Ratio = 0.32)

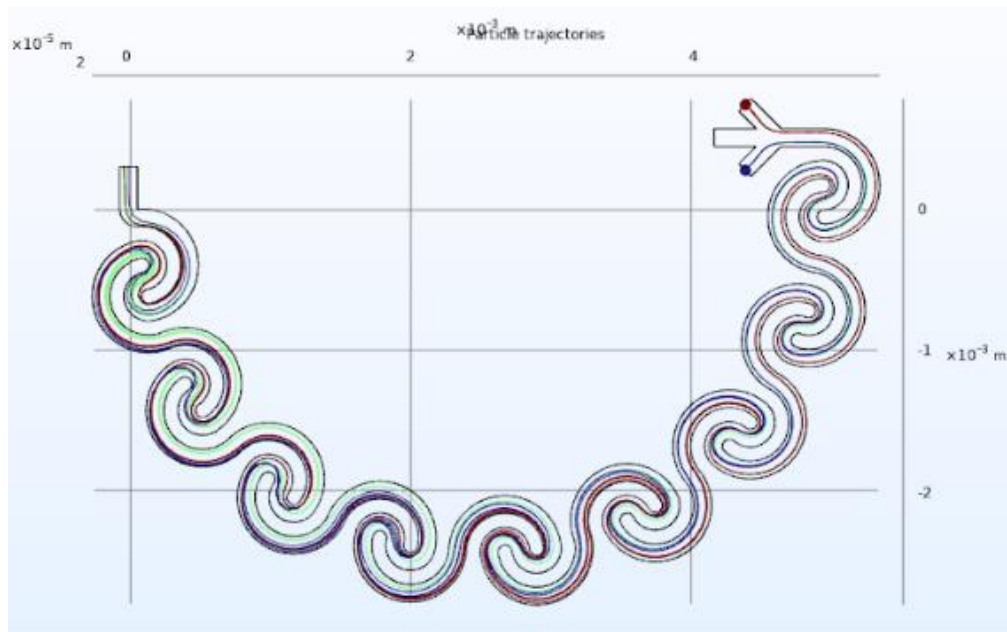
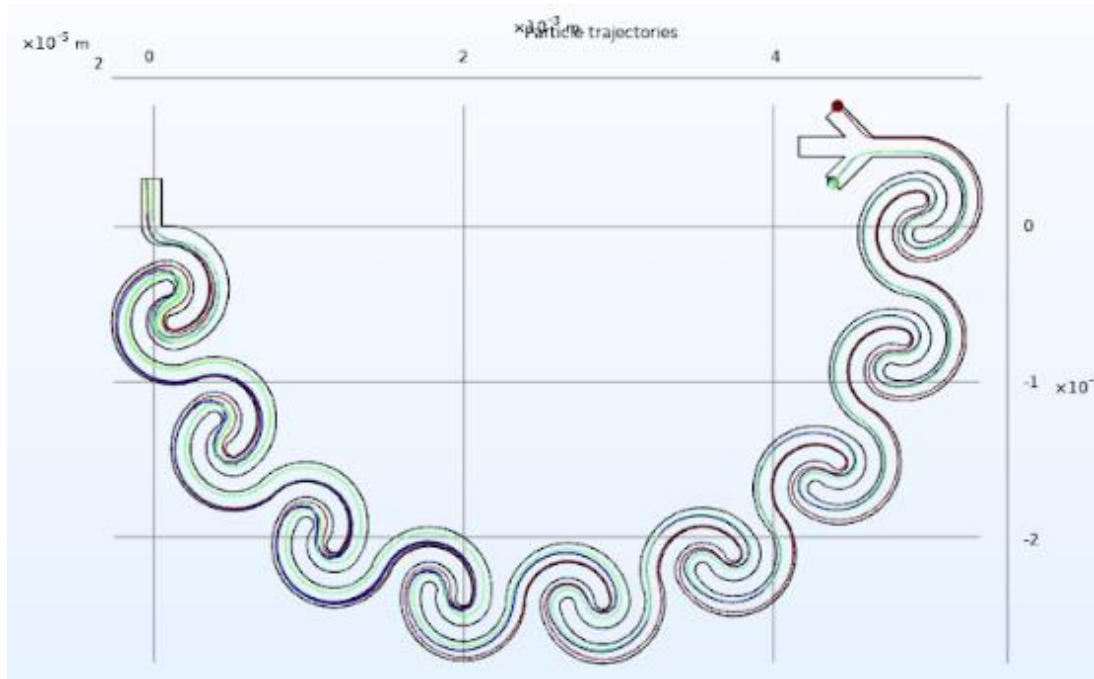


Figure 20: For fine mesh (Aspect Ratio = 0.32)



*Figure 21: For finer mesh (Aspect Ratio = 0.32)*

For coarse mesh in Figure 18 similar results were achieved as Figure 17. CTCs were separated from the other blood cells in the microchannel. Increasing the mesh quality, we observe the separation increasing between CTCs and the other blood cells. So, in Figure 19, Figure 20, Figure 21 as we improved the mesh from the coarse mesh to normal, fine and finer mesh similar kinds of results were achieved. Though there were some little differences in case of the distance between the CTCs and other particles, the difference in the distance can be said to be negligible.

For **Normal** mesh the particle trajectories are the same indicating no further changes in results with finer grids.

For our analysis the “**Normal**” mesh will be used, to save time and computational effort.

## 4.2 Effect of Varying Aspect Ratios:

In the reverse wavy microchannel the focusing position is very important. As it determines the particle trajectories. There are several parameters that are very important such as Reynolds number, dean number, lift force and dean drag force. There is another important parameter which is the ratio of inertial lift force to dean drag force.

If this ratio is less than 0.08 then the dean drag force will dominate in a flow and if the ratio is greater than 0.08 then the inertial lift force will dominate.

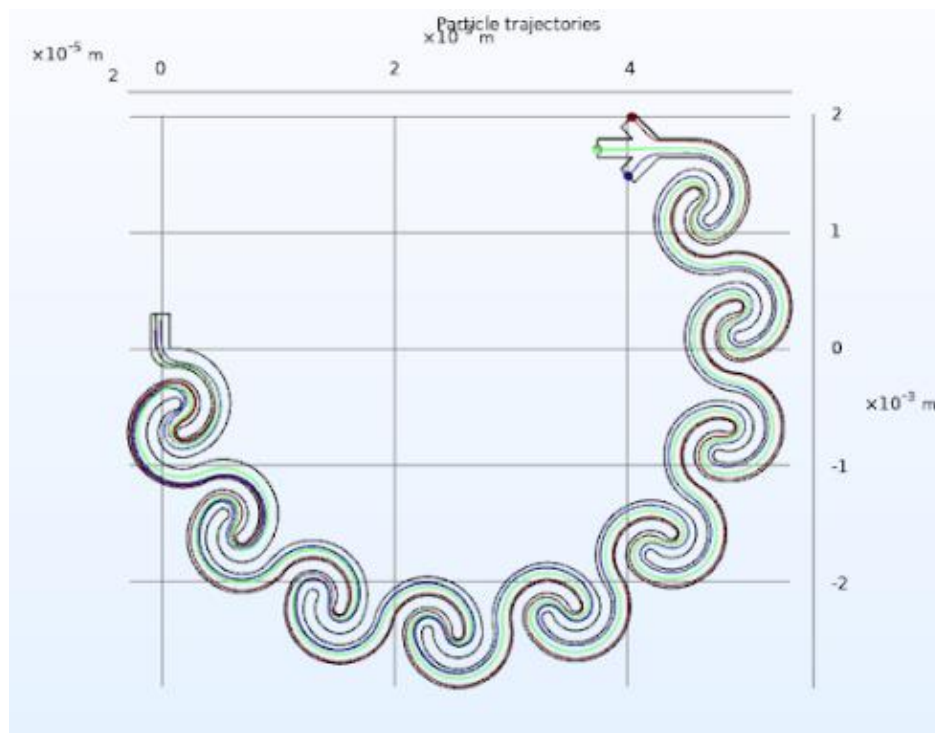
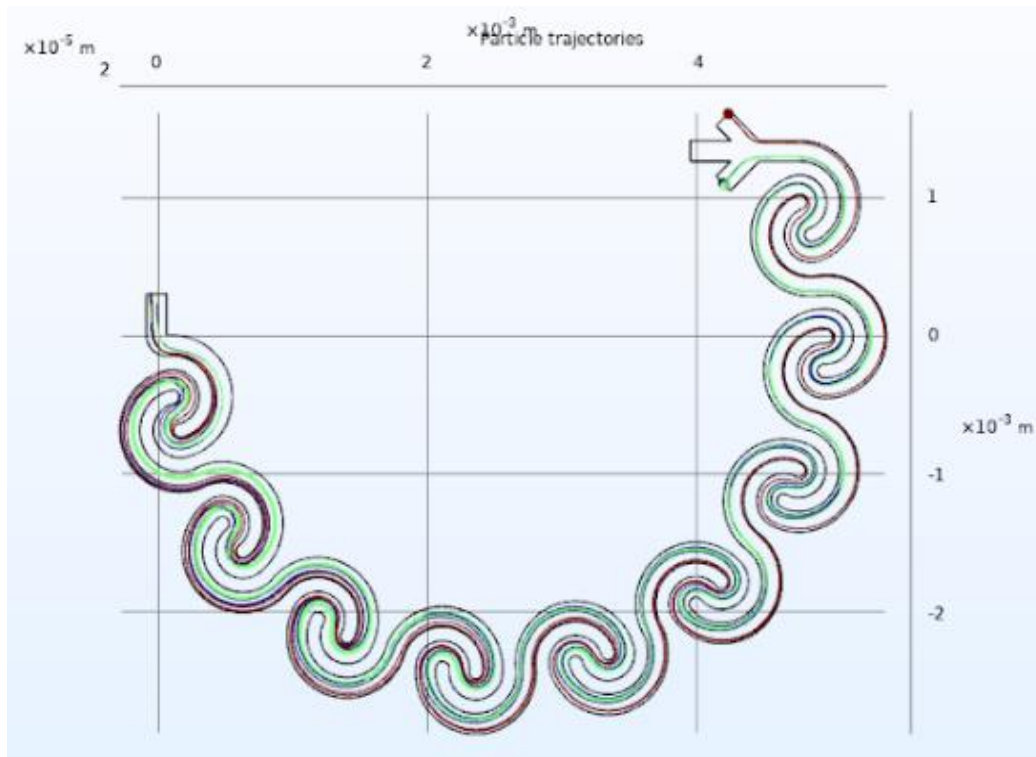


Figure 22: Particle trajectories for Aspect Ratio = 0.25



*Figure 23: Particle trajectories for Aspect Ratio = 0.27*

In Figure 22, for the  $AR = 0.25$  three different types of particles are going through three different outlets. If we increase the  $AR$  such as in Figure 23 different result was achieved. As per the simulation result 5 and 10 particles are going the lower outlet and the 15 particle is going through the upper outlet. Due to the dean flow dominating the smaller particles over inertial lift force they were going through the lower outlet. And in the case of 15 inertial lift force dominated the dean flow it goes through the upper outlet. As the  $AR$  was increased results tended to get more refined until a specific  $AR$ .

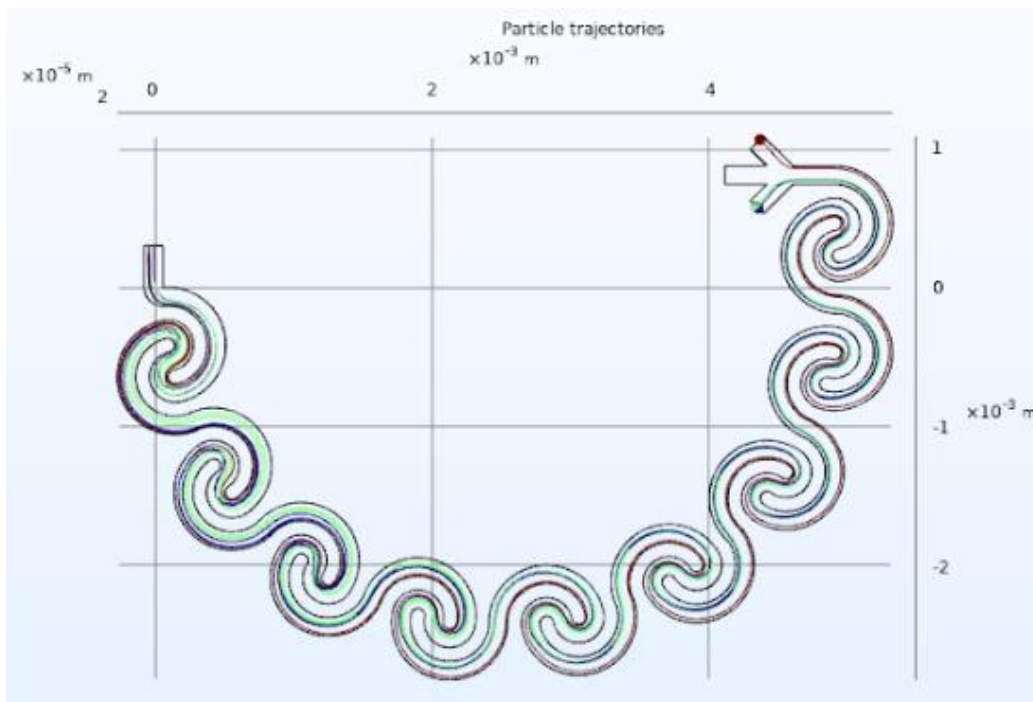


Figure 24: Particle trajectories for Aspect Ratio = 0.30

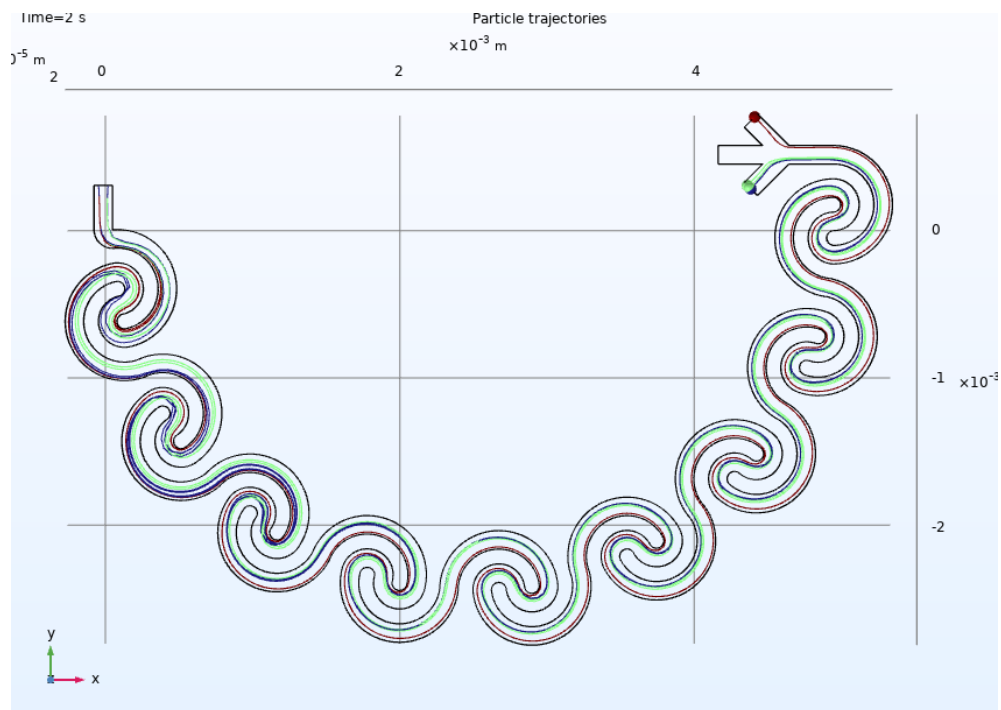
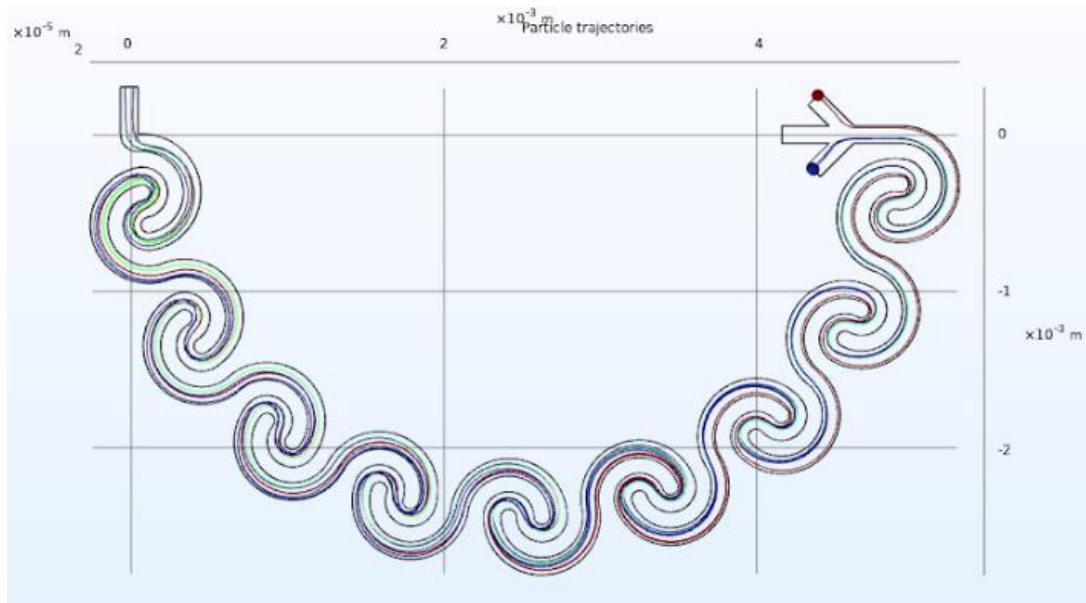


Figure 25: Particle trajectories for Aspect Ratio = 0.32



*Figure 26: Particle trajectories for Aspect Ratio = 0.36*

In Figure 24, when the AR = 0.30 the results that were achieved was more refined. The separation distance between the CTC and the other particles increased with the increase in AR. In Figure 25 the results that were achieved was approximately same as the previous condition. But the separation distance between the CTC and the other particles got increased. AR was increased again at Figure 26 and at that ratio kind of similar results was achieved but the distance between the CTCs and the other particle got little bit decreased than the previous results.

At Figure 27 same kind of results were achieved for AR = 0.39. But the distance is seen to be decreasing than the previous one. At Figure 28 the results that were achieved was very different. In the previous results it was seen that the distance was being decreased with the increasing in AR.



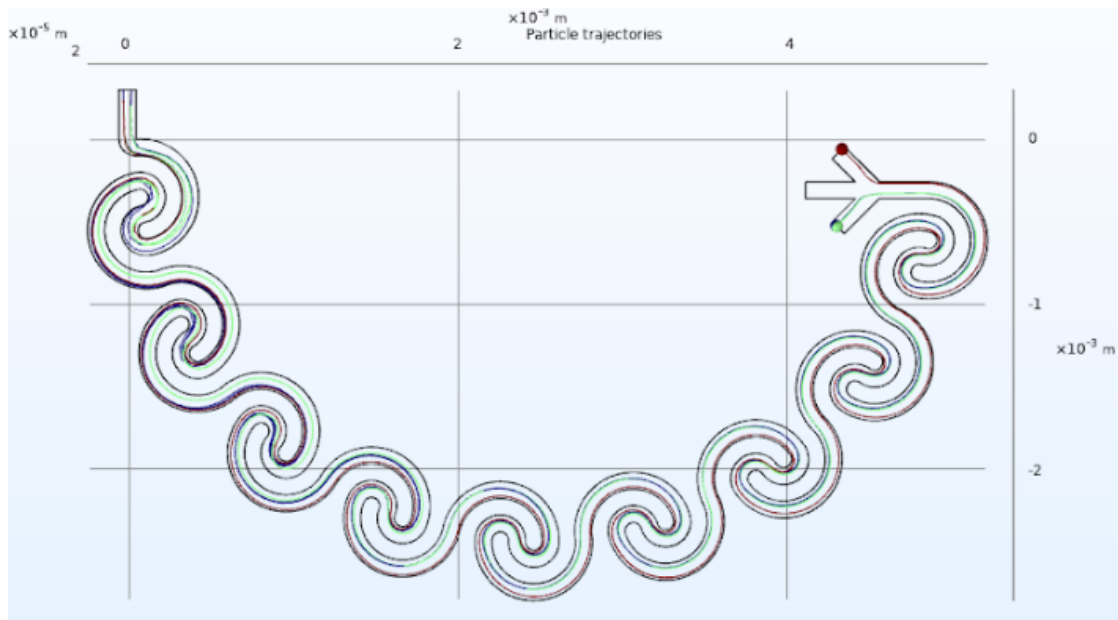


Figure 27: Particle trajectories for Aspect Ratio = 0.39

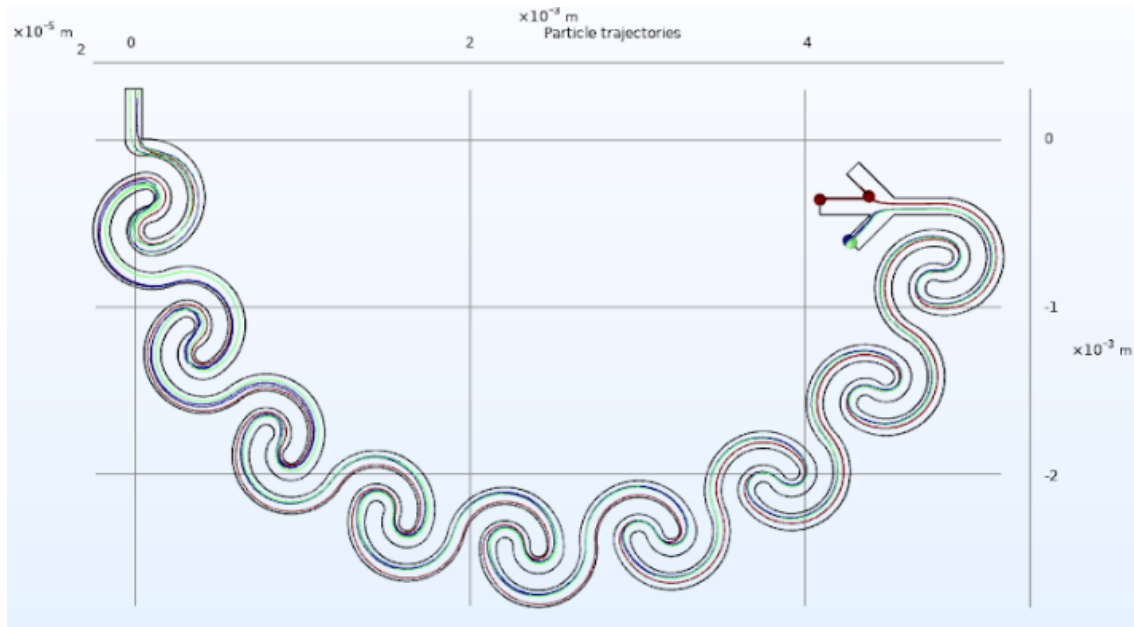


Figure 28: Particle trajectories for Aspect Ratio = 0.40

For  $AR = 0.40$  the CTCs were going through the middle outlet. After all the results are analyzed, it can be said that the maximum distance we achieved between the CTCs and the other cells was for the  $AR = 0.32$ . So, the optimum aspect ratio is **0.32**.



And for our own geometry as it is a curved channel there will be more effect of dean flow. Due to the larger diameter the 15  $\mu\text{m}$  particle will go through the upper outlet. But due to the domination of dean drag force the 3  $\mu\text{m}$  and 10  $\mu\text{m}$  particle will go through the lower outlet.

Due to smaller diameter the 3  $\mu\text{m}$  particle goes through the lower output. Then the 15  $\mu\text{m}$  particle goes through the middle.

And the lift force will dominate the 10  $\mu\text{m}$  particle that is why it goes through the first outlet

For the proposed geometry as it is a curved channel there will be more effect of dean flow. Due to the larger diameter the 15  $\mu\text{m}$  particle will go through the upper outlet. But due to the domination of dean drag force the 3  $\mu\text{m}$  and 10  $\mu\text{m}$  particle will go through the lower outlet.

### 4.3 Effect of Varying Reynold's Number:

For,  $Re = 10$  as shown in in Figure 29, no separation was achieved. The largest particles went towards the upper and middle outlet. As our objective was to separate CTCs from the other two particles with maximum distance possible so the Reynolds number will be increased gradually from 10 to 50 to see if the result is improved or not.

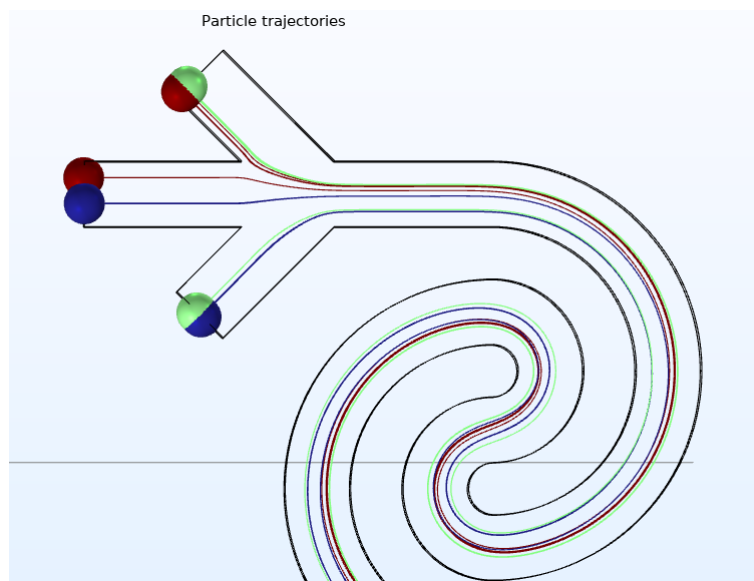
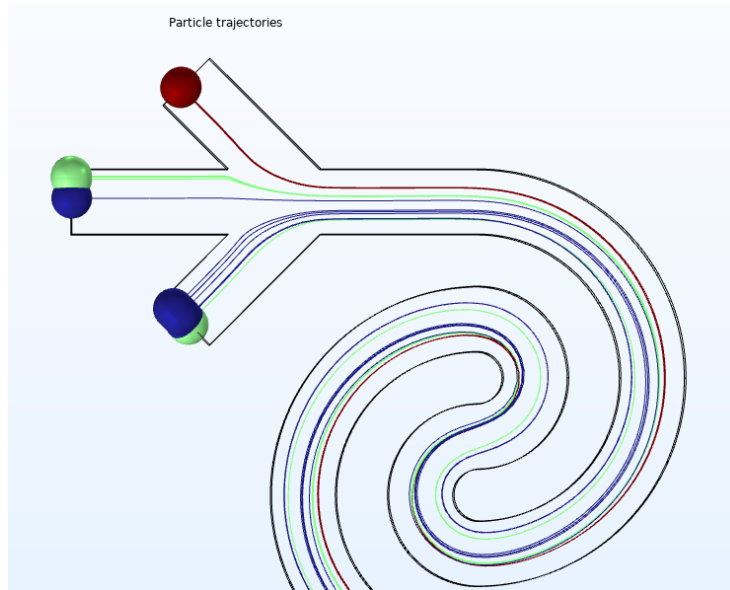
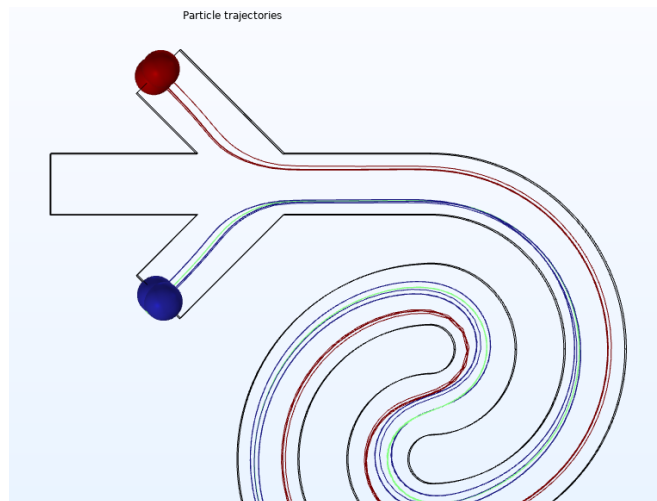


Figure 29: Particle trajectories for  $Re = 10$



*Figure 30: Particle trajectories for  $Re = 20$*



*Figure 31: Particle trajectories for  $Re = 30$*

In Figure 30 for the  $Re = 20$ , separation was achieved only for the circulating tumor cells which is going through the upper outlet. Rest of the cells (WBC and RBC) are not separated for the  $Re = 20$ .

Both of the particles were seen going through the middle and lower outlet. Our objective is satisfied as the circulating tumor cells are being separated from the rest of the cells.

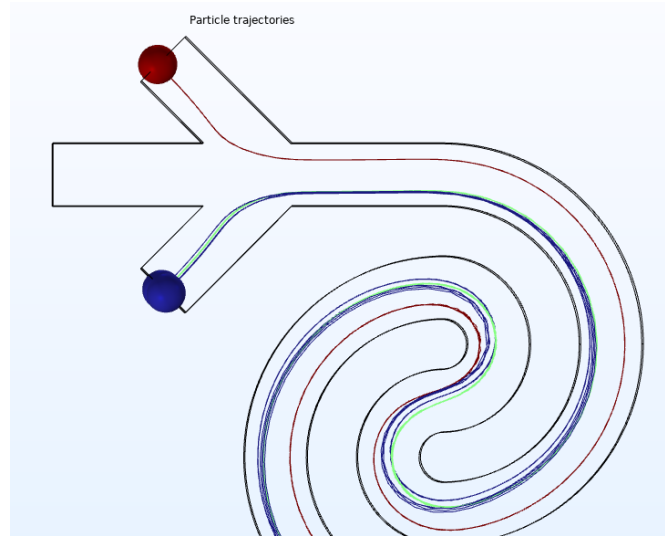


*Figure 32: Particle trajectories for  $Re = 40$*

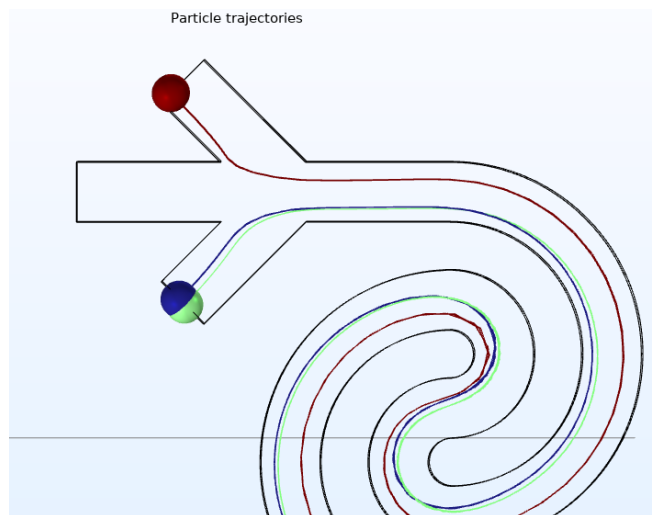


*Figure 33: Particle trajectories for  $Re = 50$*

Increasing the  $Re$ , we observe the Separation increasing between CTCs and the other blood cells. For  $Re = 30$  in Figure 31 we can see some separation of CTCs from the other two particles. The CTCs are sorted at the upper outlet and the other two went through the lower outlets. So, the

Reynolds number was increased again to see if the result is improving. And the results were improved with the increase in Reynolds number.

For  $Re = 40$  in Figure 32 same results can be seen as for the  $Re = 30$ . Though there some differences in the results. Same as the previous ones the circulating tumor cells were seen going through the upper outlet. on the other hand, the RBC and WBC were going through the lower outlet. But the lines can be seen as more refined than the previous result. So, we can say that our result is improving with the increasing of Reynolds number.

Again, the Reynolds number was increased to  $Re = 50$  in Figure 33 the same results could be seen. But a mere difference can be observed between the results of  $Re = 40$  and 50. The separation distance between the CTCs and the other cells (RBC, WBC) are greater for  $Re = 40$ . Upon analyzing it could be seen in the Figure 33 that the separation distance was reduced for  $Re = 50$ .

The RBC and WBC streams are more focused at  $Re$  of 40 and 50 and seem to merge with each other with the CTC stream remaining unchanged.

At  **$Re = 40$**  the lateral separation between the streams is largest.

Further increasing the  $Re$  to 50 causes a decrease in lateral separation, thus indicating  **$Re = 40$**  as the **Optimum Reynold's Number**.

## CHAPTER FIVE: CONCLUSIONS

### 5.1 Conclusion

The focus of this research is to employ innovative microfluidic channel designs, specifically the reverse wavy channel and circular reverse wavy channel, for the purpose of isolating circulating tumor cells (CTCs) from blood samples. Both channel configurations have been meticulously designed and fabricated. Initial experimentation with the reverse wavy channel has yielded promising results, demonstrating successful isolation of CTCs from the blood matrix.

CTC separation for Circular Reverse Wavy Channels was analyzed and **Optimum Aspect Ratio = 0.32, Optimum Re = 40** was found for the circular reverse wavy channel.

This investigation holds significant implications for the field of cancer diagnostics and therapeutics, offering the potential for enhanced CTC isolation methodologies that may ultimately contribute to improved patient outcomes. Through rigorous experimentation and analysis, our research aims to advance the understanding and application of microfluidic technologies in the context of cancer cell isolation and detection.

## **5.2 Future Scope**

### **5.2.1 Addition of Hybrid Methods such as integrating Inertial Microfluidics with DEP:**

Dielectrophoresis is a technique that allows for precise separation of the particles or cells based on their dielectric properties, also improving the efficiency of microfluidic systems. It can selectively target specific particles or cells, enhancing diagnostic assay sensitivity and specificity. Combining DEP with inertial microfluidics increases system throughput, making it suitable for high amount sample volumes. DEP is versatile, allowing handling of various particle sizes and types. It is also non-invasive, preserving sample integrity without chemical labels or physical contact. This integration can lead to more compact and integrated diagnostic devices.

### **5.2.2 Cascading Microchannels (Reverse Wavy to Spiral/Contraction-Expansion)**

Cascading microchannel is the combination of two or more same or different microchannels. The main channel can be into multiple smaller channels having a specific width and dimension. As the fluid flows through the channel the larger particles are directed into wider channels because of their size on the other hand smaller particles flow into narrower channels. Compared to other complex microfluidic separation techniques, cascading microchannels are relatively easy to fabricate and operate.

## References

- [1] D. Crosby *et al.*, “Early detection of cancer,” *Science (1979)*, vol. 375, no. 6586, Mar. 2022, doi: 10.1126/science.aay9040.
- [2] Y. Zhou, Z. Ma, and Y. Ai, “Sheathless inertial cell focusing and sorting with serial reverse wavy channel structures,” *Microsyst Nanoeng*, vol. 4, no. 1, 2018, doi: 10.1038/S41378-018-0005-6.
- [3] J. M. Martel and M. Toner, “Inertial focusing in microfluidics,” *Annu Rev Biomed Eng*, vol. 16, pp. 371–396, 2014, doi: 10.1146/annurev-bioeng-121813-120704.
- [4] L. R. Huang, E. C. Cox, R. H. Austin, and J. C. Sturm, “Continuous Particle Separation Through Deterministic Lateral Displacement,” *Science (1979)*, vol. 304, no. 5673, pp. 987–990, May 2004, doi: 10.1126/science.1094567.
- [5] K. J. Morton *et al.*, “Hydrodynamic metamaterials: Microfabricated arrays to steer, refract, and focus streams of biomaterials,” 2008. [Online]. Available: [www.pnas.org/cgi/content/full/](http://www.pnas.org/cgi/content/full/)
- [6] P. De Stefano, E. Bianchi, and G. Dubini, “The impact of microfluidics in high-throughput drug-screening applications,” May 01, 2022, *American Institute of Physics Inc.* doi: 10.1063/5.0087294.
- [7] N. Xiang and Z. Ni, “Inertial Microfluidics for Single-Cell Manipulation and Analysis,” in *Handbook of Single Cell Technologies*, Singapore: Springer Singapore, 2020, pp. 1–30. doi: 10.1007/978-981-10-4857-9\_29-1.
- [8] C. F. Rodríguez *et al.*, “Low-cost inertial microfluidic device for microparticle separation: A laser-Ablated PMMA lab-on-a-chip approach without a cleanroom,” *HardwareX*, vol. 16, p. e00493, Dec. 2023, doi: 10.1016/j.ohx.2023.e00493.

- [9] W. Tang, S. Zhu, D. Jiang, L. Zhu, J. Yang, and N. Xiang, “Channel innovations for inertial microfluidics,” *Lab Chip*, vol. 20, no. 19, pp. 3485–3502, Oct. 2020, doi: 10.1039/d0lc00714e.
- [10] J.-P. MATAS, J. F. MORRIS, and É. GUAZZELLI, “Inertial migration of rigid spherical particles in Poiseuille flow,” *J Fluid Mech*, vol. 515, pp. 171–195, Sep. 2004, doi: 10.1017/S0022112004000254.
- [11] J. A. Schonberg and E. J. Hinch, “Inertial migration of a sphere in Poiseuille flow,” *J Fluid Mech*, vol. 203, pp. 517–524, Jun. 1989, doi: 10.1017/S0022112089001564.
- [12] E. S. ASMOLOV, “The inertial lift on a spherical particle in a plane Poiseuille flow at large channel Reynolds number,” *J Fluid Mech*, vol. 381, pp. 63–87, Feb. 1999, doi: 10.1017/S0022112098003474.
- [13] B. P. Ho and L. G. Leal, “Inertial migration of rigid spheres in two-dimensional unidirectional flows,” *J Fluid Mech*, vol. 65, no. 2, pp. 365–400, Aug. 1974, doi: 10.1017/S0022112074001431.
- [14] R. G. Cox and H. Brenner, “The lateral migration of solid particles in Poiseuille flow — I theory,” *Chem Eng Sci*, vol. 23, no. 2, pp. 147–173, May 1968, doi: 10.1016/0009-2509(68)87059-9.
- [15] A. J. Chung, “A Minireview on Inertial Microfluidics Fundamentals: Inertial Particle Focusing and Secondary Flow,” *Biochip J*, vol. 13, no. 1, pp. 53–63, Mar. 2019, doi: 10.1007/s13206-019-3110-1.
- [16] Y. Gou, Y. Jia, P. Wang, and C. Sun, “Progress of Inertial Microfluidics in Principle and Application,” *Sensors*, vol. 18, no. 6, p. 1762, Jun. 2018, doi: 10.3390/s18061762.
- [17] G. SEGRÉ and A. SILBERBERG, “Radial Particle Displacements in Poiseuille Flow of Suspensions,” *Nature*, vol. 189, no. 4760, pp. 209–210, Jan. 1961, doi: 10.1038/189209a0.



- [18] D. Di Carlo, J. F. Edd, K. J. Humphry, H. A. Stone, and M. Toner, “Particle Segregation and Dynamics in Confined Flows,” *Phys Rev Lett*, vol. 102, no. 9, p. 094503, Mar. 2009, doi: 10.1103/PhysRevLett.102.094503.
- [19] J.-P. MATAS, J. F. MORRIS, and É. GUAZZELLI, “Lateral force on a rigid sphere in large-inertia laminar pipe flow,” *J Fluid Mech*, vol. 621, pp. 59–67, Feb. 2009, doi: 10.1017/S0022112008004977.
- [20] Y. Gou, Y. Jia, P. Wang, and C. Sun, “Progress of inertial microfluidics in principle and application,” Jun. 01, 2018, *MDPI AG*. doi: 10.3390/s18061762.
- [21] D. Di Carlo, “Inertial microfluidics,” 2009, *Royal Society of Chemistry*. doi: 10.1039/b912547g.
- [22] Y. Zhou, Z. Ma, and Y. Ai, “Sheathless inertial cell focusing and sorting with serial reverse wavy channel structures,” *Microsyst Nanoeng*, vol. 4, no. 1, 2018, doi: 10.1038/S41378-018-0005-6.
- [23] Y. Ying and Y. Lin, “Inertial Focusing and Separation of Particles in Similar Curved Channels,” *Sci Rep*, vol. 9, no. 1, Dec. 2019, doi: 10.1038/s41598-019-52983-z.
- [24] J. Zhu, T. J. Tzeng, and X. Xuan, “Continuous dielectrophoretic separation of particles in a spiral microchannel,” *Electrophoresis*, vol. 31, no. 8, pp. 1382–1388, Apr. 2010, doi: 10.1002/elps.200900736.
- [25] J. G. Kralj, M. T. W. Lis, M. A. Schmidt, and K. F. Jensen, “Continuous Dielectrophoretic Size-Based Particle Sorting,” *Anal Chem*, vol. 78, no. 14, pp. 5019–5025, Jul. 2006, doi: 10.1021/ac0601314.
- [26] J. Voldman, “ELECTRICAL FORCES FOR MICROSCALE CELL MANIPULATION,” *Annu Rev Biomed Eng*, vol. 8, no. 1, pp. 425–454, Aug. 2006, doi: 10.1146/annurev.bioeng.8.061505.095739.

- [27] D. R. Gossett *et al.*, “Label-free cell separation and sorting in microfluidic systems,” *Anal Bioanal Chem*, vol. 397, no. 8, pp. 3249–3267, Aug. 2010, doi: 10.1007/s00216-010-3721-9.
- [28] N. Pamme, “Continuous flow separations in microfluidic devices,” *Lab Chip*, vol. 7, no. 12, p. 1644, 2007, doi: 10.1039/b712784g.
- [29] K. Loutharback, K. S. Chou, J. Newman, J. Puchalla, R. H. Austin, and J. C. Sturm, “Improved performance of deterministic lateral displacement arrays with triangular posts,” *Microfluid Nanofluidics*, vol. 9, no. 6, pp. 1143–1149, Dec. 2010, doi: 10.1007/s10404-010-0635-y.
- [30] J. M. Martel and M. Toner, “Inertial focusing in microfluidics,” 2014, *Annual Reviews Inc.* doi: 10.1146/annurev-bioeng-121813-120704.
- [31] H. Amini, W. Lee, and D. Di Carlo, “Inertial microfluidic physics,” Aug. 07, 2014, *Royal Society of Chemistry*. doi: 10.1039/c4lc00128a.
- [32] N. Nivedita and I. Papautsky, “Continuous separation of blood cells in spiral microfluidic devices,” *Biomicrofluidics*, vol. 7, no. 5, Sep. 2013, doi: 10.1063/1.4819275.
- [33] L. Wu, G. Guan, H. W. Hou, A. Asgar. S. Bhagat, and J. Han, “Separation of Leukocytes from Blood Using Spiral Channel with Trapezoid Cross-Section,” *Anal Chem*, vol. 84, no. 21, pp. 9324–9331, Nov. 2012, doi: 10.1021/ac302085y.
- [34] S. S. Kuntaegowdanahalli, A. A. S. Bhagat, G. Kumar, and I. Papautsky, “Inertial microfluidics for continuous particle separation in spiral microchannels,” *Lab Chip*, vol. 9, no. 20, p. 2973, 2009, doi: 10.1039/b908271a.
- [35] A. A. S. Bhagat, S. S. Kuntaegowdanahalli, and I. Papautsky, “Enhanced particle filtration in straight microchannels using shear-modulated inertial migration,” *Physics of Fluids*, vol. 20, no. 10, Oct. 2008, doi: 10.1063/1.2998844.

- [36] B. Chun and A. J. C. Ladd, “Inertial migration of neutrally buoyant particles in a square duct: An investigation of multiple equilibrium positions,” *Physics of Fluids*, vol. 18, no. 3, Mar. 2006, doi: 10.1063/1.2176587.
- [37] D. Di Carlo, D. Irimia, R. G. Tompkins, and M. Toner, “Continuous inertial focusing, ordering, and separation of particles in microchannels,” *Proceedings of the National Academy of Sciences*, vol. 104, no. 48, pp. 18892–18897, Nov. 2007, doi: 10.1073/pnas.0704958104.
- [38] D. R. Gossett and D. Di Carlo, “Particle Focusing Mechanisms in Curving Confined Flows,” *Anal Chem*, vol. 81, no. 20, pp. 8459–8465, Oct. 2009, doi: 10.1021/ac901306y.
- [39] D. Di Carlo, J. F. Edd, D. Irimia, R. G. Tompkins, and M. Toner, “Equilibrium Separation and Filtration of Particles Using Differential Inertial Focusing,” *Anal Chem*, vol. 80, no. 6, pp. 2204–2211, Mar. 2008, doi: 10.1021/ac702283m.
- [40] X. Mao, I. Bischofberger, and A. E. Hosoi, “Particle focusing in a wavy channel,” *J Fluid Mech*, vol. 968, Aug. 2023, doi: 10.1017/jfm.2023.558.
- [41] J.-P. MATAS, J. F. MORRIS, and É. GUAZZELLI, “Inertial migration of rigid spherical particles in Poiseuille flow,” *J Fluid Mech*, vol. 515, pp. 171–195, Sep. 2004, doi: 10.1017/S0022112004000254.
- [42] D. Di Carlo, D. Irimia, R. G. Tompkins, and M. Toner, “Continuous inertial focusing, ordering, and separation of particles in microchannels,” *Proceedings of the National Academy of Sciences*, vol. 104, no. 48, pp. 18892–18897, Nov. 2007, doi: 10.1073/pnas.0704958104.
- [43] J. Zhou and I. Papautsky, “Fundamentals of inertial focusing in microchannels,” *Lab Chip*, vol. 13, no. 6, pp. 1121–1132, Mar. 2013, doi: 10.1039/c2lc41248a.

- [44] D. Jiang, C. Ni, W. Tang, D. Huang, and N. Xiang, “Inertial microfluidics in contraction-expansion microchannels: A review,” Jul. 01, 2021, *American Institute of Physics Inc.* doi: 10.1063/5.0058732.
- [45] T. S. Sim, K. Kwon, J. C. Park, J.-G. Lee, and H.-I. Jung, “Multistage-multiorifice flow fractionation (MS-MOFF): continuous size-based separation of microspheres using multiple series of contraction/expansion microchannels,” *Lab Chip*, vol. 11, no. 1, pp. 93–99, 2011, doi: 10.1039/C0LC00109K.
- [46] A. Al-Ali, W. Waheed, E. Abu-Nada, and A. Alazzam, “A review of active and passive hybrid systems based on Dielectrophoresis for the manipulation of microparticles,” *J Chromatogr A*, vol. 1676, p. 463268, Aug. 2022, doi: 10.1016/j.chroma.2022.463268.
- [47] S. Yan, J. Zhang, D. Yuan, and W. Li, “Hybrid microfluidics combined with active and passive approaches for continuous cell separation,” *Electrophoresis*, vol. 38, no. 2, pp. 238–249, Jan. 2017, doi: 10.1002/elps.201600386.
- [48] M. S. Islam and X. Chen, “Continuous CTC separation through a DEP-based contraction–expansion inertial microfluidic channel,” *Biotechnol Prog*, vol. 39, no. 4, Jul. 2023, doi: 10.1002/btpr.3341.